

NASA Contractor Report 178286

ICASE REPORT NO. 87-26

ICASE

ON THE NONLINEAR INTERACTION OF GÖRTLER VORTICES AND
TOLLMIE-SCHLICHTING WAVES IN CURVED CHANNEL FLOWS AT FINITE
REYNOLDS NUMBERS

Q. Isa Daudpota

Philip Hall

Thomas A. Zang

Contract Nos. NAS1-17070 and NAS1-18107

April 1987

(NASA-CR-178286) ON THE NONLINEAR
INTERACTION OF GÖRTLER VORTICES AND
TOLLMIE-SCHLICHTING WAVES IN CURVED CHANNEL
FLOWS AT FINITE REYNOLDS NUMBERS Final
Report (NASA) 63 p Avail: NTIS HC

N87-21860

Unclas
G3/02 0072172

INSTITUTE FOR COMPUTER APPLICATIONS IN SCIENCE AND ENGINEERING
NASA Langley Research Center, Hampton, Virginia 23665

Operated by the Universities Space Research Association



National Aeronautics and
Space Administration

Langley Research Center
Hampton, Virginia 23665

**ON THE NONLINEAR INTERACTION OF GÖRTLER VORTICES AND TOLLMIE-
SCHLICHTING WAVES IN CURVED CHANNEL FLOWS AT FINITE REYNOLDS NUMBERS**

Q. Isa Daudpota¹

Philip Hall²

Thomas A. Zang¹

ABSTRACT

The flow in a two-dimensional curved channel driven by an azimuthal pressure gradient can become linearly unstable due to axisymmetric perturbations and/or nonaxisymmetric perturbations depending on the curvature of the channel and the Reynolds number. For a particular small value of curvature, the critical Reynolds number for both these perturbations becomes identical. In the neighborhood of this curvature value and critical Reynolds number, nonlinear interactions occur between these perturbations. The Stuart-Watson approach is used to derive two coupled Landau equations for the amplitudes of these perturbations. The stability of the various possible states of these perturbations is shown through bifurcation diagrams. Emphasis is given to those cases which have relevance to external flows.

¹Computational Methods Branch, NASA Langley Research Center, Hampton, VA.

²Dept. of Mathematics, Exeter University, Exeter, U.K. and Institute for Computer Applications in Science and Engineering.

Research of the first author was supported by an award of a National Research Council Post-doctoral Research Associateship.

Research of the second author was supported under NASA Contract Nos. NAS1-17070 and NAS1-18107 while he was in residence at the Institute for Computer Applications in Science and Engineering (ICASE), NASA Langley Research Center, Hampton, VA 23665.

1. INTRODUCTION

In plane channel flow, instability arises due to the amplification of Tollmien-Schlichting (TS) waves. As these waves grow, they modify the mean flow, produce higher harmonics, interact with other waves, and probably produce turbulence. The initial stage of development of these waves from the linear region to the weakly nonlinear domain was analyzed by Stuart (1958) who derived the Landau equation for the temporal development of the TS wave. The presence of the cubic nonlinearity in this equation modifies the otherwise exponential variation inherent in a linear theory. This theory was able to explain the existence of an equilibrium finite amplitude perturbation in certain regions near the neutral curve.

Taylor (1923) was the first to consider the instabilities that arise due to the curvature of streamlines. He investigated the flow between two concentric cylinders due to the rotation of the inner cylinder with the outer cylinder stationary. He found that the flow becomes unstable when the parameter $Re(d/R_1)^{1/2}$ (now referred to as the Taylor number) exceeds a value of about 41. Here R_1 is the radius of the inner cylinder, d ($\ll R_1$) is the gap width of the cylinders, and Re is the Reynolds number based on the speed of the inner cylinder and d . The instability that appears as the speed of the inner cylinder exceeds the critical value is in the form of toroidal vortices. These vortices are modelled theoretically by an axisymmetric perturbation and they are stationary when they first appear.

Dean (1928) also investigated the instability in a curved channel due to the curved streamlines (see Figure 1). The flow in his experiment was generated by an azimuthal pressure gradient. The channel is formed by portions of two concentric cylinders having channel width $d \ll R_1$. Basing the Reynolds

number, Re , on the mean speed of the unperturbed flow, Dean (1928) and Walowit, Tsao, and DiPrima (1964) found that instability arises when $Re(d/R_1)^{1/2}$ exceeds a value of about 36. Here, too, as in Taylor's experiment only axisymmetric disturbances were considered.

In a detailed analysis of the linear stability of curved channel flow, Gibson and Cook (1974) argued that in a curved channel of very small curvature non-axisymmetric disturbances can play a significant role in destabilizing the mean flow. Such perturbations are analogous to TS waves in a plane channel. Their linear stability analysis shows that for channels with very small curvature, the critical Reynolds number for the TS waves is almost independent of η , ($\eta = R_1/R_2$, $R_2 =$ radius of outer wall), and it approximates very closely the corresponding value for a plane channel. The critical Reynolds number for the axisymmetric instability (Görtler vortices), on the other hand, is quite sensitive to η for η close to 1 (Figure 2). For a particular value of $\eta = \eta_c$, the critical Reynolds numbers for these instabilities are identical. For a slightly wider channel, the critical Reynolds number for the Görtler instability is lower than the almost constant critical Reynolds number for the TS perturbation. For a narrower channel, the critical Reynolds number for the Görtler instability is higher. It is, therefore, reasonable to expect that near η_c both perturbations could exist simultaneously and thereby interact with each other.

The purpose of this paper is to analyze the weakly nonlinear interaction of these two instabilities (one axisymmetric and the other non-axisymmetric) which arise when the radius ratio is nearly η_c . We use a multiple scale version of the Stuart-Watson method approach to derive the two coupled ordinary differential equations for the amplitudes of these perturbations.

While these two equations cannot be solved explicitly, they nevertheless yield significant information about the various possible bifurcations that can take place in the presence of these perturbations. Moreover, the stability properties of the equilibrium states can be deduced.

When considering a growing boundary layer, a self-consistent analysis of wave interactions within it requires the application of the triple deck theory as shown by Hall and Smith (1984). In channel flows, however, we do not need to consider the effects of boundary layer growth, thereby greatly simplifying the analysis while still giving a qualitative picture of what might happen in an unbounded flow. It is in this context that we wish to study the Görtler/TS interaction in a curved channel. This study may be viewed as an extension of the work of Gibson and Cook (1974) into the weakly nonlinear regime.

2. MEAN FLOW AND PERTURBATION EQUATIONS

Let (r, θ, z) be the cylindrical coordinates with the axis of the concentric walls along the z -axis and R_1 and R_0 the radii of the inner and outer cylinder respectively (see Figure 1).

When the flow between the concentric walls is maintained by a constant azimuthal pressure gradient $\frac{\partial P}{\partial \theta}$ (< 0), the solution of the momentum equations yields

$$U(r) = W(r) = 0, \quad (2.1)$$

where $U(r)$ and $W(r)$ are the radial and axial mean velocities, respectively. The azimuthal velocity is given explicitly by

$$V(r) = \frac{R_o}{2\nu\rho} \frac{\partial P}{\partial \theta} \left[r \log r + \frac{\eta^2 \log \eta}{r(1-\eta^2)} (r^2 - 1) \right], \quad (2.2)$$

$$(\eta \leq r \leq 1)$$

where ν and ρ are the kinematic viscosity and density, respectively, and $\eta = R_i/R_o$. Here the distance from the axis is normalized with respect to R_o , so that r varies from η at the inner radius to 1 at the outer radius.

A channel with small curvature will behave locally like a plane channel, and for it the azimuthal velocity $V(r)$ should approach the familiar parabolic shape. As η approaches 1, the velocity

$$V(r) = - \frac{R_o}{2\nu\rho} \frac{\partial P}{\partial \theta} [(1 - \eta)^2 \zeta(1 - \zeta)] \quad (2.3)$$

$$= V_m \zeta(1 - \zeta), \quad 0 \leq \zeta \leq 1 \quad (2.4)$$

where
$$V_m = - \frac{R_o}{2\nu\rho} \frac{\partial P}{\partial \theta} (1 - \eta)^2 \quad (2.5)$$

and ζ is given by

$$r = (1 - \eta)\zeta + \eta. \quad (2.6)$$

Thus ζ varies from 0 to 1 as r varies from η to 1. Note that in this limit, V_m is four times the center line velocity.

Based on (2.3), (2.4), (2.5), and (2.6), (2.2) can be simply expressed as

$$V(r) = V_m f(r) \quad (2.7)$$

where

$$f(r) = -\frac{1}{(1-\eta)^2} \left[r \log r + \frac{\eta^2 \log \eta}{r(1-\eta)^2} (r^2 - 1) \right]. \quad (2.8)$$

The fully nonlinear disturbance equations for the radial velocity u , azimuthal velocity v , axial velocity w , and the continuity equation are as follows:

$$\begin{aligned} \frac{\partial p}{\partial \zeta} = & -\frac{(1-\eta)}{\text{Re}} \frac{1}{r} \partial_{\theta} \left(\frac{\partial v}{\partial \zeta} \right) - \frac{1}{\text{Re}^2} \partial_z \left(\frac{\partial w}{\partial \zeta} \right) \\ & + \left(-\frac{(1-\eta) \partial_t}{\text{Re}} + \frac{(1-\eta)^2}{\text{Re}^2 r^2} \partial_{\theta\theta} + \frac{1}{\text{Re}^2} \partial_{zz} - \frac{f(r)}{r} \frac{(1-\eta)}{\text{Re}} \partial_{\theta} \right) u \end{aligned} \quad (2.9)$$

$$\begin{aligned} & + \left(-\frac{(1-\eta)^2}{\text{Re}} \frac{2}{r^2} \partial_{\theta} + \frac{2}{r} f(r) (1-\eta) + \frac{(1-\eta)^2}{r^2} \frac{1}{\text{Re}} \partial_{\theta} \right) v \\ & - (1-\eta) \left[\frac{v}{\text{Re} r} \partial_{\theta} u - \frac{v^2}{r} + \frac{1}{\text{Re}^2 (1-\eta)} \left\{ u \frac{\partial u}{\partial \zeta} + w \partial_z u \right\} \right], \end{aligned}$$

$$\begin{aligned} \frac{\partial^2 v}{\partial \zeta^2} = & \frac{\text{Re}}{r} (1-\eta) \partial_{\theta} p - \frac{1}{r} (1-\eta) \frac{\partial v}{\partial \zeta} \\ & + \left[-\frac{1}{\text{Re}} \frac{2}{r^2} (1-\eta)^2 \partial_{\theta} + (1-\eta) \frac{df(r)}{dr} + (1-\eta) \frac{f(r)}{r} \right] u \\ & + \left[\text{Re} (1-\eta) \partial_t + \frac{(1-\eta)^2}{r^2} \partial_{\theta\theta} - \partial_{zz} + \text{Re} \frac{f(r)}{r} (1-\eta) \partial_{\theta} \right. \\ & \left. + \frac{1}{r^2} (1-\eta)^2 \right] v \end{aligned} \quad (2.10)$$

$$+ (1-\eta) \left[\frac{u}{(1-\eta)} \frac{\partial v}{\partial \zeta} + \text{Re} \frac{v}{r} \partial_{\theta} v + \frac{uv}{r} + \frac{w}{(1-\eta)} \partial_z v \right],$$

$$\begin{aligned} \frac{\partial^2 w}{\partial \zeta^2} &= \text{Re}^2 \partial_z p - \frac{(1-\eta)}{r} \frac{\partial w}{\partial \zeta} \\ &+ \left[\text{Re}(1-\eta) \partial_t - \frac{(1-\eta)^2}{r^2} \partial_{\theta\theta} - \partial_{zz} + \text{Re}(1-\eta) \frac{f(r)}{r} \partial_\theta \right] w \quad (2.11) \\ &+ (1-\eta) \text{Re} \frac{v}{r} \partial_\theta w + u \frac{\partial w}{\partial \zeta} + w \partial_z w, \end{aligned}$$

and

$$\frac{\partial u}{\partial \zeta} = - \frac{(1-\eta)}{r} u - \frac{\text{Re}}{r} (1-\eta) \partial_\theta v - \partial_z w \quad (2.12)$$

where the quantities that appear in (2.9), (2.10), (2.11) and (2.12) are non-dimensionalized versions of primed physical quantities shown below:

Pressure $p = \frac{\hat{p}}{\rho V_m^2}$

Radial position $r = r'/R_0 = (1-\eta)\zeta + \eta, \quad \eta \leq r \leq 1$
 $0 \leq \zeta \leq 1$

Axial position $z = z'/d$

Azimuthal position $\theta = \theta'$

Time $t = t' / \left(\frac{R_0}{V_m} \right)$

Radial velocity $u = u' / \left(\frac{V}{d} \right)$

Axial velocity $w = w' / \left(\frac{V}{d} \right)$

Azimuthal velocity $v = v'/V_m$.

Note that u' and w' are scaled with respect to the diffusive velocity scale while v' is scaled with respect to the convective velocity scale. The mean flow is $(0, V_m f(r), 0)$ and the nondimensionalized perturbation is (u, v, w) in the (r, θ, z) direction. The Reynolds number

$$Re = V_m d/\nu,$$

where $d = R_0 - R_1$.

The effect of the purely azimuthal (non-axisymmetric) and the purely axial (axisymmetric) perturbation can be modelled by a general expression for the perturbation proportional to $\exp[\sigma t + i(kz + m\theta)]$ where the non-dimensional axial wave number $k = k'd$, the non-dimensional azimuthal wave number $m = m'$, and the non-dimensional complex growth rate

$\sigma = \sigma' / \left(\frac{V_m}{R_0}\right) = \sigma_R + i \sigma_I$. The partial derivatives $\partial_t, \partial_z, \partial_\theta$ can now be replaced by σ, ik, im respectively within the linear part of the equations (2.9) to (2.12).

The four equations of motion can be written as a set of six first-order ordinary differential equations, as was done by Eagles (1971). Thus we write

$$\left(p, \frac{\partial v}{\partial z}, \frac{\partial w}{\partial z}, u, v, w\right)^T \equiv \underline{q} \quad (2.13)$$

so that the equations can be written as

$$\frac{\partial}{\partial z} \underline{q} = \underline{\Phi} \underline{q} + \underline{n} \quad (2.14)$$

where \mathbf{q} is a 6×6 matrix representing the linear contribution and \mathbf{n} is a six element vector containing the nonlinear terms. The last three elements of the vectors \mathbf{q} and \mathbf{n} are zero at the two channel walls. The terms representing the linear and nonlinear contributions will be discussed in the next section after an explicit expression for \mathbf{q} is given.

3. PERTURBATION EXPANSION FOR NONLINEAR WAVE INTERACTION

The perturbation to the mean flow is expressed in the form:

$$\begin{aligned}
 \mathbf{q} = & \epsilon \{ (\underline{A} E + \underline{B} F) + \text{c.c.} \} \\
 & + \epsilon^2 \{ (\underline{C} E^2 + \underline{D} F^2 + \underline{G} EF^* + \underline{H} EF) + \text{c.c.} \} \\
 & + \epsilon^2 \{ \underline{J} E^0 + \underline{K} F^0 \} \\
 & + \epsilon^3 \{ (\underline{L} E^3 + \underline{M} F^3 + \underline{N} E^2 F^* + \underline{P} E^2 F \\
 & \quad + \underline{Q} EF^2 + \underline{R} E^* F^2) + \text{c.c.} \} \\
 & + \epsilon^3 \{ (\underline{S} E + \underline{T} F) + \text{c.c.} \} + O(\epsilon^4),
 \end{aligned} \tag{3.1}$$

where \mathbf{q} is the perturbation vector given by (2.13), c.c. represents the complex conjugate of the terms in the preceding parentheses, ϵ is a small expansion parameter, * represents complex conjugation.

The vector

$$\underline{A} = (a_1, a_2, a_3, a_4, a_5, a_6)^T \quad (3.2)$$

represents the Görtler perturbation,

$$\underline{B} = (b_1, b_2, b_3, b_4, b_5, b_6)^T \quad (3.3)$$

represents the TS perturbation,

$$E = \exp(ikz), \quad (3.4a, b)$$

$$F = \exp(im\theta)\exp(\sigma t),$$

and

$$\sigma = \sigma_R + i\sigma_I. \quad (3.5)$$

$\underline{A} E$ and $\underline{B} F$ represent the Görtler and TS instabilities respectively. Other terms represent higher harmonics and the mean flow modification which arise due to the quadratic nonlinearity in the equations.

The amplitude coefficients \underline{C} , \underline{D} , \underline{G} , and \underline{H} are due to the direct interaction between the TS and the Görtler instabilities. As self interaction occurs for each of these instabilities, the mean flow profile itself becomes modified through the generation of effects represented by \underline{J} and \underline{K} . The terms at order ϵ^3 arise due to the interactions of the terms of order ϵ^2 and the Görtler and TS perturbations.

As will become clear later, it will not be necessary to solve for the unknown coefficients at order ϵ^3 . By using the solvability condition for

the equations governing S and T, the evolution equations for the amplitude of the Görtler (A) and of the TS (B) waves can be found. The method of multiple-scales used in this paper for obtaining these evolution equations follows closely that suggested by Matkowsky (1970).

Throughout, we will require that the last three components of the vectors A to T are zero at the two curved walls in order to satisfy the zero velocity boundary conditions.

For the perturbation expansion (3.1), the appropriate slower time variable is τ defined by

$$\tau = \epsilon^2 t, \quad (3.6)$$

where ϵ is the same small expansion parameter used earlier. This gives

$$\frac{\partial}{\partial t} \rightarrow \frac{\partial}{\partial t} + \epsilon^2 \frac{\partial}{\partial \tau}. \quad (3.7)$$

The Reynolds number Re is expanded about a value R_0 on the neutral stability curve so that

$$Re = R_0 + \epsilon^2 R_1. \quad (3.8)$$

Hence,

$$1/Re \approx 1/R_0 - \frac{R_1}{R_0^2} \epsilon^2 \quad (3.9)$$

and

$$1/Re^2 \approx 1/R_0^2 - 2 \frac{R_1}{R_0^3} \epsilon^2. \quad (3.10)$$

Returning to (3.1), we now regard all the vectors A to T as functions of both ζ and τ . For example:

$$\underline{A} \rightarrow \underline{A}(\zeta) X(\tau)$$

$$\underline{B} \rightarrow \underline{B}(\zeta) Y(\tau)$$

which states that in the neighborhood of the neutral stability curve the solutions for the linear problem, $\underline{A}(\zeta)$ and $\underline{B}(\zeta)$, adequately represent the shape of the perturbations in the weakly nonlinear regime. The amplitudes of these perturbations, $X(\tau)$ and $Y(\tau)$, depend on the slowly varying time variable τ .

The remaining vectors can be represented similarly, e.g.,

$$\underline{C} \rightarrow \underline{C}(\zeta) X^2(\tau)$$

$$\underline{H} \rightarrow \underline{H}(\zeta) X(\tau) Y(\tau).$$

Henceforth, when referring to vectors \underline{A} to \underline{K} we will only be considering their spatial dependence because it can be shown that the temporal dependence cancels out throughout the equations for these vectors.

By substituting (3.1) and (3.7) to (3.10) into (2.13), we obtain an equation for \underline{q} of the form:

$$\begin{aligned} \frac{\partial}{\partial \zeta} \underline{q} &= \underline{L}_1 [\partial_z, \partial_\theta] \underline{q} + \underline{T}_1 [\partial_t] \underline{q} \\ &+ \epsilon^2 \underline{L}_2 [\partial_z, \partial_\theta] \underline{q} \\ &+ \epsilon^2 \underline{T}_{21} [\partial_t] \underline{q} + \epsilon^2 \underline{T}_{22} [\partial_\tau] \underline{q} \\ &+ \underline{N}_1 [\partial_z, \partial_\theta] \{ \underline{q} \otimes \underline{q} \} \\ &+ \epsilon^2 \underline{N}_2 [\partial_z, \partial_\theta] \{ \underline{q} \otimes \underline{q} \} . \end{aligned} \tag{3.11}$$

$L_1, L_2, T_1, T_{21}, T_{22}$ are linear operators, equivalent to 6×6 matrices. Their dependence on the differential operators $\partial_z, \partial_\theta, \partial_t$ and ∂_τ is indicated within the square brackets. Both $\underline{N}_1[\partial_z, \partial_\theta] \{q \otimes q\}$ and $\underline{N}_2[\partial_z, \partial_\theta] \{q \otimes q\}$ represent nonlinear terms containing the operators ∂_z and ∂_θ . $\{q \otimes q\}$ symbolizes quadratic terms comprised of the components of q . Here onwards we shall refer to $\underline{N}_1[\partial_z, \partial_\theta] \{q \otimes q\}$ by \underline{N}_1 . Since in the analysis of (3.11) we will only be concerned with terms of $O(\epsilon^3)$, it will not be necessary to consider the term $\epsilon^2 \underline{N}_2[\partial_z, \partial_\theta] \{q \otimes q\}$ which is $O(\epsilon^4)$. The elements of the operators are given explicitly in Appendix A.

To determine the linear stability problem for the Görtler and the TS perturbations acting individually, terms of $O(\epsilon)$ need to be considered. From these terms, those with coefficient E will give the linear stability perturbation equations for the Görtler disturbance. Similarly, the terms with coefficient F will give the equations for the TS disturbance.

At $O(\epsilon)$

(i) The terms with coefficient E give

$$\frac{dA}{d\zeta} = L_1[ik, 0]A + T_1[0]A \quad (3.12)$$

for the Görtler perturbation.

(ii) The terms with coefficient F give

$$\frac{dB}{d\zeta} = L_1[0, im]B + T_1[i\sigma_I]B \quad (3.13)$$

for the Tollmien-Schlichting perturbation.

From these equations, vectors A and B can be determined. Note the difference in the parameters of the operators in (i) and (ii), particularly the fact that $\partial_t = 0$ for the Görtler while for the TS, $\partial_t = i\sigma_I$. In both cases we are considering neutrally stable perturbations.

When collecting terms of $O(\epsilon^2)$ for determining vectors C to K, the operators L_2, T_{21}, T_{22} can be neglected because when they operate on q, contributions of $O(\epsilon^2)$ are produced. As these operators are already pre-multiplied by ϵ^2 , the net contribution from these terms will be $O(\epsilon^4)$ and hence negligible. In the equations for C to K that follow, the non-linear contributions are contained in N₁. Of the six elements of the vector representing the contribution from N₁, only the first three (n_1, n_2, n_3) are non-zero, and these are listed following each equation. The discussion following (3.5) gives the physical basis for presence of the vectors C to K.

At $O(\epsilon^2)$

(i) The terms with coefficient E^2 give

$$\frac{dC}{d\zeta} = L_1 [2ik, 0] \underline{C} + T_1 [0] \underline{C} + \text{nonlinear contribution from } \underline{N}_1, \quad (3.14)$$

where

$$n_1 = -(1 - \eta) \left\{ -\frac{a_4^2}{R_0^2 r} - a_5^2 / r \right\}$$

$$\begin{aligned} n_2 &= a_4 a_2 + a_4 a_5 (1 - \eta) + ik a_6 a_5 \\ n_3 &= a_4 a_3 + ik a_6^2. \end{aligned}$$

(ii) The terms with coefficient F^2 give

$$\frac{d\underline{D}}{d\underline{\zeta}} = \underline{L}_1 [0, 2im] \underline{D} + \underline{T}_1 [2 i\sigma_I] \underline{D} + \text{nonlinear contribution from } \underline{N}_1, \quad (3.15)$$

where

$$\begin{aligned} n_1 &= (1 - \eta) \left\{ \frac{b_4^2}{R_0^2 r} - \frac{b_5^2}{r} \right\} \\ n_2 &= (1 - \eta) \left\{ \frac{b_4 b_2}{(1-\eta)} + \frac{imb_5^2 R_0}{r} + \frac{b_4 b_5}{r} \right\} \\ n_3 &= (1 - \eta) \frac{R_0}{r} im b_5 b_6 + b_3 b_4. \end{aligned}$$

(iii) The terms with coefficient EF^* give

$$\frac{d\underline{G}}{d\underline{\zeta}} = \underline{L}_1 [ik, -im] \underline{G} + \underline{T}_1 [-i\sigma_I] \underline{G} + \text{nonlinear contribution from } \underline{N}_1, \quad (3.16)$$

where

$$\begin{aligned} n_1 &= (1 - \eta) \left\{ \frac{2a_4 b_4^*}{R_0^2 r} - \frac{im a_4 b_5}{R_0 r} + \frac{ik b_4^* a_6}{R_0^2 (1-\eta)} - \frac{ik b_6^* a_4}{R_0^2 (1-\eta)} + \frac{im a_5 b_4^*}{R_0 r} + \frac{2a_5 b_5^*}{r} \right\} \\ n_2 &= (1 - \eta) \left\{ \frac{a_4 b_2^* + b_4^* a_2}{(1-\eta)} - \frac{im R_0 a_5 b_5^*}{r} + \frac{a_4 b_5^* + b_4^* a_5}{r} + \frac{ik a_5 b_6^*}{(1-\eta)} \right\} \\ n_3 &= -im(1 - \eta) R_0 a_5 b_6^* + a_4 b_3^* + b_4^* a_3 + ik b_6^* a_6. \end{aligned}$$

(iv) The terms with coefficient EF give

$$\frac{dH}{d\zeta} = L_1 [ik, im] \underline{H} + T_1 [i\sigma_I] \underline{H} + \text{nonlinear contribution from } \underline{N}_1, \quad (3.17)$$

where

$$n_1 = -(1 - \eta) \left[\begin{array}{cc} -\frac{1}{R_0^2 r} 2a_4 b_4 - \frac{1}{R_0 r} a_4 im b_5 - \frac{1}{R_0^2 (1-\eta)} b_4 ika_6 + \frac{1}{R_0^2 (1-\eta)} b_6 ika_4 & \\ + \frac{a_5 im b_4}{R_0 r} & - \frac{2 a_5 b_5}{r} \end{array} \right]$$

$$n_2 = R_0 (1 - \eta) \left\{ \frac{a_4 b_2 + b_4 a_2}{R_0 (1-\eta)} + \frac{a_5 im b_5}{r} + \frac{a_4 b_5 + b_4 a_5}{R_0 r} + \frac{b_6 ika_5}{(1-\eta)R_0} \right\}$$

$$n_3 = \frac{R_0 (1-\eta)}{r} im a_5 b_6 + a_4 b_3 + b_4 a_3 + ik a_6 b_6 .$$

(v) The terms with coefficient E⁰ give

$$\frac{dJ}{d\zeta} = L_1 [0,0] \underline{J} + T_1 [0] \underline{J} + \text{nonlinear contribution from } \underline{N}_1, \quad (3.18)$$

where

$$n_1 = \frac{2(1-\eta)}{R_0 r} a_4 a_4^* + \frac{2ik}{R_0^2} \{a_4^* a_6 - a_4 a_6^*\} + \frac{2(1-\eta)}{r} a_5 a_5^*$$

$$n_2 = a_4 a_2^* + a_4^* a_2 + \frac{(1-\eta)}{r} (a_4 a_5^* + a_4^* a_5) + ik(a_5 a_6^* - a_5^* a_6)$$

$$n_3 = a_4 a_3^* + a_4^* a_3 .$$

(vi) The terms with coefficient F⁰ give

$$\frac{dK}{d\zeta} = L_1[0,0]K + T_1[0]K + \text{nonlinear contribution from } \underline{N}_1, \quad (3.19)$$

where

$$n_1 = 2(1-\eta) \left\{ \frac{b_4 b_4^*}{2R_0 r} + \frac{im}{R_0 r} (b_4^* b_5 - b_4 b_5^*) + b_5 b_5^* \right\}$$

$$n_2 = b_4 b_2^* + b_4^* b_2 + \frac{(1-\eta)}{r} \{b_4 b_5^* + b_4^* b_5\}$$

$$n_3 = \frac{R_0(1-\eta)}{r} \{imb_5^* b_6 - imb_5 b_6^*\} + b_4 b_3^* + b_4^* b_3.$$

So far we have collected terms with coefficient ϵ and obtained the equations for the spatial dependence of the neutrally stable Görtler and TS perturbations followed by collecting terms that have coefficient ϵ^2 . At $O(\epsilon^3)$, we will see that only equations of \underline{S} and \underline{T} need to be considered for obtaining the time evolution of the Görtler and TS amplitudes. \underline{S} and \underline{T} are functions of ζ and τ . In the following, we shall again revert to writing the Görtler and TS perturbations as $\underline{A} X(\tau)$ and $\underline{B} Y(\tau)$ respectively, with \underline{A} and \underline{B} dependent only on ζ . It will be seen from the form of the equations for \underline{S} and \underline{T} that the temporal dependence does not cancel out; indeed, it is this very property that allows us to get time evolution equations for $X(\tau)$ and $Y(\tau)$.

Collecting terms of $O(\epsilon^3)$ with coefficient E , and with coefficient F , we obtain the equations for \underline{S} and \underline{T} :

$$\begin{aligned} \frac{\partial \underline{S}}{\partial \zeta} = & L_1[ik,0]\underline{S} + T_1[0]\underline{S} \\ & + L_2[ik,0]\underline{A} X(\tau) + T_{21}[0]\underline{A} X(\tau) + T_{22}[\partial_\tau]\underline{A} X(\tau) \end{aligned} \quad (3.20)$$

+ contribution from \underline{N}_1

and

$$\frac{\partial \underline{T}}{\partial \zeta} = \underline{L}_1 [0, im] \underline{T} + \underline{T}_1 [i\sigma_I] \underline{T}$$

$$+ \underline{L}_2 [0, im] \underline{B} Y(\tau) + \underline{T}_{21} [i\sigma_I] \underline{B} Y(\tau) + \underline{T}_{22} [\partial_\tau] \underline{B} Y(\tau) \quad (3.21)$$

+ contribution from \underline{N}_1 .

The contributions from \underline{N}_1 to both these equations involve a very large number of terms and are therefore not written explicitly at this stage. They will however appear in the final equations for $X(\tau)$ and $Y(\tau)$.

The homogeneous parts of (3.20) and (3.21) are the same as those of (3.12) and (3.13) for \underline{A} and \underline{B} respectively. In order that the non-homogeneous equations (3.20) and (3.21) have solutions, the nonhomogeneous parts of these equations should be orthogonal to the adjoint column vectors $\tilde{\underline{A}}$ and $\tilde{\underline{B}}$ respectively. These vectors are solutions of the following equations:

$$\frac{d\tilde{\underline{A}}}{d\zeta} = -[\underline{L}_1 [ik, 0] + \underline{T}_1 [0]]^T \tilde{\underline{A}} \quad (3.22)$$

$$\frac{d\tilde{\underline{B}}}{d\zeta} = -[\underline{L}_1 [0, im] + \underline{T}_1 [i\sigma_I]]^T \tilde{\underline{B}} \quad (3.23)$$

where $\tilde{\underline{A}}^T = (\tilde{a}_1, \tilde{a}_2, \tilde{a}_3, \tilde{a}_4, \tilde{a}_5, \tilde{a}_6)$ and $\tilde{\underline{B}}^T = (\tilde{b}_1, \tilde{b}_2, \tilde{b}_3, \tilde{b}_4, \tilde{b}_5, \tilde{b}_6)$. Unlike the boundary conditions for the equations for \underline{A} and \underline{B} where the last three of their components are zero, here the first three components of $\tilde{\underline{A}}$ and $\tilde{\underline{B}}$ are zero at the boundaries.

Using the orthogonality condition, we obtain the following equations for $X(\tau)$ and $Y(\tau)$:

$$\int_0^1 d\zeta [\tilde{\underline{A}}^T \underline{L}_2[ik,0] \underline{A} X(\tau) + \tilde{\underline{A}}^T \cdot \underline{T}_{22}[\partial_\tau] \underline{A} X(\tau) + \tilde{\underline{A}}^T \cdot (\text{contribution from } \underline{N}_1)] = 0 \quad (3.24)$$

and

$$\int_0^1 d\zeta [\tilde{\underline{B}}^T \underline{L}_2[0,im] \underline{B} Y(\tau) + \tilde{\underline{B}}^T \underline{T}_{21}[i\sigma_I] \underline{B} Y(\tau) + \tilde{\underline{B}}^T \underline{T}_{22}[\partial_\tau] \underline{B} Y(\tau) + \tilde{\underline{B}}^T \cdot (\text{contribution from } \underline{N}_1)] = 0. \quad (3.25)$$

The terms representing $(\tilde{\underline{A}}^T \cdot \text{contribution from } \underline{N}_1)$ and $(\tilde{\underline{B}}^T \cdot \text{contribution from } \underline{N}_1)$ are given in Appendix B. After integrating over ζ , these equations can be written as

$$\frac{d X(\tau)}{d\tau} = R_1 \beta_1 X(\tau) + \delta_1 X(\tau) |X(\tau)|^2 + \eta_1 X(\tau) |Y(\tau)|^2 \quad (3.26)$$

and

$$\frac{d Y(\tau)}{d\tau} = R_1 \beta_2 Y(\tau) + \delta_2 Y(\tau) |X(\tau)|^2 + \eta_2 Y(\tau) |Y(\tau)|^2 \quad (3.27)$$

where β_i, δ_i , and η_i , ($i = 1, 2$), are coefficients obtained from (3.24) and (3.25). R_1 is a measure of the deviation from the neutral stability curve as is given by (3.8). It appears in (3.26) and (3.27) because it is a common factor in matrix \underline{L}_2 in (3.24) and (3.25). Equations (3.26) and (3.27) are the coupled Landau equations which determine the time evolution of the amplitudes of the Görtler and TS perturbations. The analysis of these equations will be presented after the next section. The following section gives a brief

description of the numerical method used for obtaining the coefficients A to K in (3.1). All the terms in the perturbation expansion have been verified by using the symbolic manipulation language MACSYMA.

4. COMPUTATION OF THE COEFFICIENTS

The equations governing the ζ dependence of the coefficients A to K are given in the previous section. A and B are described by a set of homogeneous ordinary differential equations while the equations for the remaining amplitudes are nonhomogeneous.

A fourth-order finite difference scheme (Malik, Chuang, and Hussaini (1982)) was used to solve these equations. For details of the method, the reader may refer to Malik, et al. (1982) and Hall and Malik (1986). The calculations were performed on a nonuniform grid which clusters the points near the walls. A suitable distribution of grid points was obtained using the relation

$$\zeta_i = (\sin(\pi x_i/2) + 1)/2, \quad (4.1)$$

where

$$x_i = \frac{1}{N-1} [2i - 1 - N], \quad 1 \leq i \leq N \quad (4.2)$$

and

N = total number of grid points.

In order to determine the vectors A to K to 3 digit accuracy, 51 grid points were sufficient for the range of Reynolds number and wave numbers that we considered.

The coefficients of the Landau equations derived in the last section are functions of the vectors \underline{A} to \underline{K} . These vectors become dependent on the slow time variable τ only when we perturb the flow from its neutrally stable state. In the neighborhood of the neutral stability curves for the Görtler and TS perturbations, the shape of the vectors (as functions of ζ) remains unchanged, and hence we only need to consider the shapes of the neutrally stable modes.

The familiar neutral stability curves for the linear Görtler and TS perturbations are presented in Figures 3 and 4, respectively. Here, the generally accepted convention of labelling one of the arms of the stability curve as "lower" and the other as "upper" is used. To analyze the different kinds of possible interactions between a Görtler and a TS perturbation at an arbitrary Reynolds number R_0 consider the schematic diagram of Figure 5. (Refer to this figure and its caption for the abbreviations GL, GU, TSL, TSU used in what follows.) A Görtler perturbation GL with wave number k_1 and Reynolds number Re slightly different from R_0 ($Re = R_0 + \epsilon^2 R_1$) can interact with a TS wave with the same Reynolds number but with wave numbers m_1 or m_2 corresponding to TSL and TSU respectively. Similarly, GU with wave number k_2 can interact with either TSL or TSU. So, in all there are four possible interactions.

It can be seen from Figure 2 that for $\eta = R_1/R_2 = \eta_c = 2.179 \times 10^{-5}$, the critical Reynolds number for the Görtler and TS perturbations is $8 \times 5772.2 \approx 46176$ where 5772.2 is the critical Reynolds number for a plane channel flow based on half channel width and centerline velocity (Orszag (1971)). It is for this value of η that we compute the amplitudes \underline{A} to \underline{K} for $46176 \leq R_0 \leq 120,000$. This range is probably sufficient to

reveal the possible interactions. Results for other values of η in the neighborhood of η_c can be obtained using a simple argument that we will present in the next section.

The components of \underline{A} to \underline{K} for each value of R_0 are used to compute the coefficients $\beta_1, \delta_1, \eta_1, \beta_2, \delta_2,$ and η_2 of the two Landau equations. For computing these coefficients, vectors \underline{A} and \underline{B} need to be normalized. This was done by dividing \underline{A} by its centerline azimuthal component (centerline value of a_5), and dividing \underline{B} by its centerline radial velocity component (centerline value of b_4). Since β_1 and δ_1 do not depend on the presence of a TS perturbation, each of these has a unique value for each point on the neutral stability curve. When both GL and GU are considered for a fixed Reynolds number, β_1 and δ_1 will each have different values on the two arms of the neutral stability wave, corresponding to the different wave numbers. A similar argument applies to β_2 and η_2 which are independent of the Görtler perturbation. These coefficients will be further discussed in the next section.

5. SOLUTION OF THE LANDAU EQUATIONS

In this section, we analyze the possible interactions by studying the properties of the coupled Landau equations. These properties are displayed in the form of bifurcation diagrams which show the amplitudes of the equilibrium states and their stability properties.

Equations (3.26) and (3.27) can be written in terms of $|X|^2$ and $|Y|^2$:

$$\frac{1}{2} \frac{d|X|^2}{dt} = \mu \beta_{1R} |X|^2 + \delta_{1R} |X|^2 |X|^2 + \eta_{1R} |X|^2 |Y|^2 \quad (5.1)$$

$$\frac{1}{2} \frac{d|Y|^2}{dt} = \mu \beta_{2R} |Y|^2 + \delta_{2R} |Y|^2 |X|^2 + \eta_{2R} |Y|^2 |Y|^2 \quad (5.2)$$

where β_{1R} , β_{2R} , δ_{1R} , δ_{2R} , η_{1R} , and η_{2R} are real parts of the corresponding Landau coefficient, e.g., $\beta_2 = \beta_{2R} + i\beta_{2I}$. It is found that β_1 is real and so $\beta_1 = \beta_{1R}$. By suitably scaling the amplitudes X and Y it is possible to make $\delta_1 = -1$ and $|\eta_2| = 1$ so as to facilitate the analysis of the equations. For notational convenience, we replace R_1 in (3.26) and (3.27) by μ in the above equations. From here on we shall drop the subscript R because all the coefficients of the equations are real.

The growth rates with respect to τ (for $\mu = 1$) of the Görtler (β_1) and TS (β_2) perturbations are shown in Figure 6 and Figure 7 respectively. In Figure 7 it should be noted that the negative values of β_2 corresponds to TSU in Figure 4.

There are two graphs each for η_1 and δ_2 depending on the types of possible interaction between a Görtler and TS wave. Figure 8a shows η_1 versus Reynolds number for the interaction of GL with TSL and TSU and Figure 8b displays the same variables for the interaction of GU with TSL and TSU. Figures 9a and 9b give graphs for δ_2 for the same interactions as given in Figures 8a and 8b. Figure 10 shows a graph of Reynolds number versus η_2 .

The graphs of the coefficient of the Landau equation mentioned in the last two paragraphs have been computed for $(1 - \eta) = (1 - \eta_c) = 2.179 \times 10^{-5}$, which corresponds to a channel with very small curvature and one for which the critical Reynolds number for the Görtler and TS perturbations are identical. In what follows we will extend the analysis to channels for η in the neighborhood of η_c .

In (5.1) and (5.2) the coefficients of $|X|^2$ and $|Y|^2$ are $\mu\beta_1$ and $\mu\beta_2$ respectively, which shows that the linear growth rates of $|X|^2$ and $|Y|^2$ are proportional to the deviation μ from R_0 (Reynolds number $= R_0 + \epsilon^2\mu$). Similarly, it is reasonable to assume a linear dependence of

the growth rate on the deviation from the radius ratio η_c . If we write $(1 - \eta) = (1 - \eta_c) + \varepsilon^2 v$ as a perturbation from $(1 - \eta_c)$, and take ε to be the expansion parameter given by (3.8), the growth rates of $|X|^2$ and $|Y|^2$ would also be linearly dependent on v . The effect of the deviation from $(1 - \eta_c)$ on the coefficients of the nonlinear terms of the Landau equations is of a higher order than we are concerned with and so we shall only consider its effect on the growth rate through the parameter v .

Equations (5.1) and (5.2) can now be written as

$$\frac{1}{2} \frac{d|X|^2}{d\tau} = (\mu\beta_1 + v\gamma_1) |X|^2 + \delta_1 |X|^2 |X|^2 + \eta_1 |X|^2 |Y|^2 \quad (5.3)$$

$$\frac{1}{2} \frac{d|Y|^2}{d\tau} = (\mu\beta_2 + v\gamma_2) |Y|^2 + \delta_2 |Y|^2 |X|^2 + \eta_2 |Y|^2 |Y|^2. \quad (5.4)$$

The zero-growth rate curves for $|X|^2$ and $|Y|^2$ are straight lines in the (v, μ) plane, passing through the origin and having slopes of $(-\gamma_1/\beta_1)$ and $(-\gamma_2/\beta_2)$ respectively. Numerical computations show the first slope to be of order -10^9 and the second to be approximately zero; therefore in what follows, we take $\gamma_2 = 0$. To compute these slopes, the wave numbers for the Gortler and TS waves were fixed at their values for $\mu = 0, v = 0$, which is equivalent to $R = Re_c$ and $(1 - \eta) = (1 - \eta_c)$. The slopes were found for this neighborhood for these fixed wave numbers. As can be expected, the slopes are of the same order of magnitude as those of the curves for the critical Reynolds number versus $(1 - \eta)$ given by Gibson and Cook (see Figure 2). Note that the wave numbers change along their curves, while in our case we keep them constant. We computed the change in Reynolds number with change in $(1 - \eta)$ at the cross-over point shown in Figure 2.

There are four possible steady state solutions to (5.3) and (5.4):

$$(i) \quad |X|^2 = 0, \quad |Y|^2 = 0 \quad (5.5a,b)$$

$$(ii) \quad |Y|^2 = 0, \quad |X|^2 = -\frac{\beta_1}{\delta_1} \left(\mu + \frac{\nu\gamma_1}{\beta_1} \right) \quad (5.6a,b)$$

$$(iii) \quad |X|^2 = 0, \quad |Y|^2 = -\frac{\beta_2}{\eta_2} \mu \quad (5.7a,b)$$

$$(iv) \quad |X|^2 = \left[-\eta_1 \beta_2 \mu + \eta_2 \beta_1 \left(\mu + \frac{\nu\gamma_1}{\beta_1} \right) \right] / (\eta_1 \delta_2 - \delta_1 \eta_2) \quad (5.8a)$$

$$|Y|^2 = \left[-\delta_2 \beta_1 \left(\mu + \frac{\nu\gamma_1}{\beta_1} \right) + \delta_1 \beta_2 \mu \right] / (\eta_1 \delta_2 - \delta_1 \eta_2) . \quad (5.8b)$$

To assess the stability of these states, it is necessary to linearize the equations about these states. The reader may refer to Boyce and DiPrima (1977) for a discussion of the stability analysis of such coupled equations.

Table 1 summarizes the values of β_i, η_i , and $\delta_i, i = 1, 2$, for the four possible interactions. This tabulation is mainly to facilitate the analysis and discussion of these interactions; other values can be obtained from the graphs for these quantities. This table of results can be used to show that many possible equilibrium states exist depending on the Reynolds number. Here we shall concentrate on the three cases which we believe to be of most practical importance. The bifurcation pictures for the other cases can be found in say Keener (1976) or Guckenheimer and Holmes (1984).

The three cases we consider are:

(a) Interaction of Görtler and TS waves for $\eta = \eta_c + \epsilon^2 \nu$ and

$Re = Re_c + \varepsilon^2 \mu$. Here we consider the cases when the Reynolds number is at or very close to the critical value for both perturbations, and with wave numbers corresponding to the critical Reynolds number and its vicinity. Representative values for this case can be found near the end of each of Sections A - D in Table 1.

(b) Interaction of TSL with GL.

(c) Interaction of TSL with GU.

Case (a): In this case, it is found that $\eta_1/\eta_2 > \beta_1/\beta_2 > \delta_1/\delta_2$, $\delta_i < 0$, $\eta_i > 0$, $\beta_i > 0$ for $i = 1, 2$. For $\nu > 0$, the Görtler mode is the most unstable on the basis of linear theory and for $\nu < 0$ the TS wave is the most unstable.

The solution (5.5a,b) exists for all values of μ whilst (5.6a,b) and (5.7a,b) exist for $\mu > -\nu\gamma_1/\beta_1$ and $\mu < 0$ respectively. The mixed mode solution (5.8a,b) can exist for either a finite, zero or semi-infinite range of values of μ depending on $\beta_i, \eta_i, \delta_i$. In the present case, we find that if $\nu < 0$, the mixed mode does not exist. However, for $\nu > 0$ the mixed mode exists for a finite range of values of μ including the origin. The bifurcation diagrams for this case are shown in Figures (11a,b). In these figures, continuous and broken lines correspond to stable and unstable solutions of the Landau equations respectively. We note that the TS mode can never be in stable equilibrium without the presence of a Görtler mode. In contrast to this situation, the Görtler mode can exist alone and be stable to small perturbations. However, the finite amplitude states in these figures are unstable to sufficiently large perturbations. This instability leads to $|X|$ and $|Y|$ terminating in a finite time singularity as in the

case for a TS wave in a straight channel. Thus, the threshold amplitude phenomenon of Meksyn and Stuart (1951) persists in the presence of Görtler vortices. It is not possible to quantify the effect of the Görtler mode on the threshold amplitude. However, a phase plane analysis of the Landau equations shows that the Görtler mode significantly reduces the size of the finite amplitude perturbation required to induce the finite time breakdown of the equations. In that sense, the Görtler mode has a significant effect on the subcritical breakdown of the TS waves. However, for a sufficiently low level of background noise, we should expect that a stationary Görtler mode could be set up by slowly increasing the Reynolds number.

Case (b): Here we consider the interaction of TSL with GL. In this situation, other modes of instability can occur at lower Reynolds number but since this situation is relevant to the corresponding external boundary layer problem we believe it to be of some importance. This is because in this case, as in Case (c), the TS wave now bifurcates supercritically and the possibility of stable mixed mode solutions must now be investigated. Here we concentrate on the interaction of such a mode with a GL vortex. Case (c) will be concerned with the interaction with a GU vortex.

The parameters $\delta_1, \delta_2, \eta_1,$ and η_2 are all negative and satisfy

$$\delta_1/\delta_2 < \beta_1/\beta_2 < \eta_1/\eta_2, \quad (\beta_i > 0, i = 1,2).$$

A routine calculation lead to the bifurcation pictures shown in Figures (12a,b). We see that the mixed mode always bifurcates from the "pure-mode" which is the least unstable on the basis of linear theory. This bifurcation

leaves the pure-mode stable so that at sufficiently large μ , both pure modes are possible stable equilibrium states. However, in the absence of any finite amplitude background noise we expect that the pure mode which is the most unstable on the basis of linear theory would be set up when the Reynolds number is gradually increased.

Case (c): Here we consider the interaction of TSL and GU. For this case $\delta_1, \delta_2, \eta_2$ are negative whilst η_1 is positive. The relationship between the ratios of the coefficients is:

$$\delta_1/\delta_2 < \beta_1/\beta_2 < -\eta_1/\eta_2, \quad (\beta_i > 0, i = 1,2).$$

The bifurcation pictures are shown in Figures (13a,b). If the Görtler mode is the most unstable on the basis of linear theory, then there is no secondary bifurcation and the TS mode is never stable. When the TS wave bifurcates first, then it is initially stable before it suffers a secondary bifurcation to a stable mixed mode. The mixed mode then meets the "pure" Görtler mode which changes from being unstable to stable. Thus, for both $v > 0$ and $v < 0$ at sufficiently large values of μ the only stable state possible is that corresponding to a finite amplitude Görtler vortex. Hence, the Görtler mode effectively prevents the finite amplitude growth of the TS wave.

6. CONCLUSIONS

In this paper we have considered the interaction of two types of perturbations in a curved channel flow; these are the travelling nonaxisymmetric

wave (TS) and the axisymmetric vortical perturbation referred to as the Görtler vortices.

By using the Stuart-Watson approach, two coupled equations for the amplitudes of TS and the Görtler perturbations were obtained. Coefficients of these equations have been calculated for their interaction, from Reynolds number starting at the common critical value Re_c for both the perturbations up to a large enough value which we think covers all the possible interactions. We have, however, concentrated our attention on those interactions which we think are significant in external flows.

We have seen in the previous section that for R close to Re_c the only possible stable "pure state" to be Görtler vortices. For a finite range of Reynolds numbers, a mixed mode is possible, but in any experimental investigation of this problem, we expect this range to be too small to be detected. However, the threshold amplitude effect associated with a finite amplitude TS wave remains intact and indeed is augmented by the curvature. In external flows such as a Blasius boundary layer or an attachment line boundary layer, this effect, if repeated, would make these flows more sensitive to background noise.

Consideration of the interaction between a TS perturbation corresponding to the lower branch of its neutral curve with a Görtler perturbation belonging to the lower branch of its neutral curve, shows that a stable finite amplitude perturbation of either type can be set up depending on which one is most linearly unstable. The value of the radius ratios η determines which of the perturbations is most unstable.

For the interaction of the TS perturbation corresponding to the lower arm of its neutral stability curve with the Görtler perturbation corresponding to

the upper arm of its neutral stability curve, we find that the Görtler vortex prevents the occurrence of a finite amplitude TS wave far from the neutral curve. When a TS wave is the most linearly unstable of the two perturbations, a finite amplitude TS wave develops, the amplitude of which increases as the Reynolds number increases further from its value on the neutral curve until a "mixed" mode appears. Here both the TS and Görtler have finite amplitudes. As Reynolds number increases further, the mixed mode bifurcates into a stable Görtler mode. In the case when the Görtler mode is the most linearly unstable, only a finite amplitude Görtler state is possible as the Reynolds number increases from a value on the neutral curve.

For external flows, an asymptotically self-consistent description of non-linear TS waves has been given by Smith (1979). Here the disturbance was described by "Triple Deck" theory and the streamwise scaling for the TS wave corresponds to lower branch TS waves in our problem. Further it was shown that lower branch TS waves bifurcate supercritically so we can expect that our results for the interaction of TS waves and Görtler vortices in channel might have implications to the external flow problem. Of course, the effect of boundary layer growth might negate the validity of us drawing these conclusions, however, we believe that our calculations show what is the likely effect of the possible interactions involving TS waves and Görtler vortices.

In a later publication, we will report the numerical simulations of the interaction in curved channel flow between such perturbations.

7. ACKNOWLEDGEMENT

Q.I.D. would like to thank Dr. Mujeeb Malik of High Tech. Corporation for his help and encouragement during the course of this work. The help of Dr. Sandra Deloach of Norfolk State University is also gratefully acknowledged. She helped to verify the terms in the perturbation expansions through the use of the symbolic manipulation language MACSYMA.

APPENDIX A

Here the nonzero components of the operators of (3.11) are given explicitly in terms of their row-column location, i.e., (1,2) will refer to element in first row and second column.

$L_1[\partial_z, \partial_\theta]$ is a 6×6 matrix:

$$(1,2) = -\frac{(1-\eta)}{R_0} \frac{1}{r} \partial_\theta$$

$$(1,3) = -\frac{\partial_z}{R_0^2}$$

$$(1,4) = \frac{(1-\eta)^2}{R_0^2 r^2} \partial_{\theta\theta} + \frac{\partial_{zz}}{R_0^2} - \frac{f(r)}{r} \frac{(1-\eta)}{R_0} \partial_\theta$$

$$(1,5) = -\frac{2(1-\eta)^2}{R_0 r^2} \partial_\theta + \frac{2}{r} f(r)(1-\eta) + \frac{(1-\eta)^2}{r^2 R_0} \partial_\theta$$

$$(2,1) = \frac{R_0(1-\eta)}{r} \partial_\theta$$

$$(2,2) = -\frac{(1-\eta)}{r}$$

$$(2,4) = -\frac{2(1-\eta)^2}{R_0 r^2} \partial_\theta + \frac{df(r)}{dr} (1-\eta) + \frac{f(r)}{r} (1-\eta)$$

$$(2,5) = (1-\eta)^2/r^2 - \frac{(1-\eta)^2}{r^2} \partial_{\theta\theta} - \partial_{zz} + R_0 \frac{f(r)}{r} (1-\eta) \partial_\theta$$

$$(3,1) = R_0^2 \partial_z$$

$$(3,3) = -(1 - \eta)/r$$

$$(3,6) = -\frac{(1-\eta)^2}{r^2} \partial_{\theta\theta} - \partial_{zz} + R_0(1 - \eta)\frac{f(r)}{r} \partial_{\theta}$$

$$(4,4) = -(1 - \eta)/r$$

$$(4,5) = -\frac{R_0(1-\eta)}{r} \partial_{\theta}$$

$$(4,6) = -\partial_z$$

$$(5,2) = (6,3) = 1.$$

$T_1[\partial_t]$ is a 6×6 matrix:

$$(1,4) = -\frac{(1-\eta)}{R_0} \partial_t$$

$$(2,5) = (3,6) = R_0(1 - \eta)\partial_t.$$

$L_2[\partial_z, \partial_{\theta}]$ is a 6×6 matrix:

$$(1,2) = (1 - \eta) \frac{R_1}{R_0^2 r} \partial_{\theta}$$

$$(1,3) = \frac{2 R_1}{R_0^3} \partial_z$$

$$(1,4) = -\frac{2}{R_0^3} R_1 \frac{(1-\eta)^2}{r^2} \partial_{\theta\theta} - 2 \frac{R_1}{R_0^3} \partial_{zz} + \frac{f(r)}{r} (1-\eta) \frac{R_1}{R_0^2} \partial_{\theta}$$

$$(1,5) = (1-\eta)^2 \frac{R_1}{R_0^2} \cdot \frac{2}{r^2} \partial_{\theta} - \frac{(1-\eta)^2}{r^2} \frac{R_1}{R_0^2} \partial_{\theta}$$

$$(2,1) = \frac{R_1}{r} (1-\eta) \partial_{\theta}$$

$$(2,4) = \frac{R_1}{R_0^2} \frac{2}{r^2} (1-\eta)^2 \partial_{\theta}$$

$$(2,5) = R_1 \frac{f(r)}{r} (1-\eta) \partial_{\theta}$$

$$(3,1) = 2 R_0 R_1 \partial_z$$

$$(3,6) = R_1 (1-\eta) \frac{f(r)}{r} \partial_{\theta}$$

$$(4,5) = -\frac{R_1}{r} (1-\eta) \partial_{\theta}.$$

$\mathbf{T}_{21}[\partial_t]$ is a 6×6 matrix:

$$(1,4) = \frac{R_1}{R_0^2} (1-\eta) \partial_t$$

$$(2,5) = R_1 (1-\eta) \partial_t$$

$$(3,6) = R_1 (1-\eta) \partial_t.$$

$\mathbf{T}_{22}[\partial_\tau]$ is a 6×6 matrix:

$$(1,4) = -\frac{(1-\eta)}{R_0} \partial_\tau$$

$$(2,5) = (3,6) = R_0(1-\eta)\partial_\tau.$$

$\mathbf{N}_1[\partial_z, \partial_\theta] \{\underline{q} \otimes \underline{q}\}$ is a 6 component column vector:

$$(1,1) = -(1-\eta) \left[\frac{v}{R_0 r} \partial_\theta u - \frac{v^2}{r} + \frac{1}{R_0^2(1-\eta)} \{w \partial_z u - u \partial_z w\} - \frac{1}{R_0^2 r} \{u^2 + u \partial_\theta v\} \right]$$

$$(2,1) = (1-\eta) \left[\frac{u}{(1-\eta)} \frac{\partial v}{\partial \zeta} + R_0 \frac{v}{r} \partial_\theta v + \frac{uv}{r} + \frac{w}{(1-\eta)} \partial_z v \right]$$

$$(3,1) = R_0(1-\eta) \frac{v}{r} \partial_\theta w + u \frac{\partial w}{\partial \zeta} + w \partial_z w.$$

APPENDIX B

Here we give the nonlinear terms of $O(\epsilon^3)$ which form part of the coupled Landau equations. Note the presence of cubic terms such as $|X(\tau)|^2 X(\tau)$, etc. The lower case letters are elements of the vectors given in capitals, e.g., $\underline{G} = (g_1, g_2, g_3, g_4, g_5, g_6)^T$. Each of these elements are functions of ζ .

(i) $\tilde{\underline{A}} \cdot$ (contribution from \underline{N}_1) =

$$\begin{aligned}
 & \left(\frac{1-\eta}{r}\right) [2j_5 a_5 + 2c_5 a_5^*] X(\tau) |X(\tau)|^2 \tilde{a}_1 \\
 & + \frac{(1-\eta)}{r} [c_4 a_5^* + c_5 a_4^* + j_4 a_5 + j_5 a_4] X(\tau) |X(\tau)|^2 \tilde{a}_2 \\
 & + [-ik c_6 a_5^* + 2ik a_6^* c_5 + j_6 ika_5] X(\tau) |X(\tau)|^2 \tilde{a}_2 \\
 & + [c_4 a_2^* + a_4^* c_2 + j_4 a_2 + a_4 j_2] X(\tau) |X(\tau)|^2 \tilde{a}_2 \\
 & + \frac{1}{R_0^2} [-ik c_4 a_6^* + 2ik a_4^* c_6 + j_4 ika_6] X(\tau) |X(\tau)|^2 \tilde{a}_1 \\
 & + \frac{2(1-\eta)}{R_0^2 r} [c_4 a_4^* + j_4 a_4] X(\tau) |X(\tau)|^2 \tilde{a}_1 \\
 & - \frac{1}{R_0^2} [-ik c_6 a_4^* + 2ik a_6^* c_4 + j_6 ika_4] X(\tau) |X(\tau)|^2 \tilde{a}_1 \\
 & + [(c_4 a_3^* + a_4^* c_3) + (j_4 a_3 + a_4 j_3)] X(\tau) |X(\tau)|^2 \tilde{a}_3
 \end{aligned}$$

$$\begin{aligned}
 & + [-ik c_6 a_6^* + 2ik a_6^* c_6 + j_6 ika_6] X(\tau)|X(\tau)|^2 \tilde{a}_3 \\
 & - \frac{(1-\eta)}{R_0 r} [-im h_4 b_4^* + b_5^* im h_4 + g_5 im b_4 - im b_5 g_4] X(\tau)|Y(\tau)|^2 \tilde{a}_1 \\
 & \quad + [b_6^* ik h_5 + b_6 ik g_5 + ik a_5 k_6] X(\tau)|Y(\tau)|^2 \tilde{a}_2 \\
 & + R_0 \frac{(1-\eta)}{r} [-im h_5 b_5^* + b_5^* im h_5 + g_5 im b_5 - im b_5 g_5] X(\tau)|Y(\tau)|^2 \tilde{a}_2 \\
 & \quad + \frac{(1-\eta)}{r} [h_4 b_5^* + b_4^* h_5 + g_4 b_5 + b_4 g_5 + a_4 k_5 + a_5 k_4] X(\tau)|Y(\tau)|^2 \tilde{a}_2 \\
 & \quad + [h_4 b_2^* + b_4^* h_2 + g_4 b_2 + b_4 g_2 + a_2 k_4 + a_4 k_2] X(\tau)|Y(\tau)|^2 \tilde{a}_2 \\
 & + \frac{R_0 (1-\eta)}{r} [-im h_5 b_6^* + b_5^* im h_6 + g_5 im b_6 - im b_5 g_6] X(\tau)|Y(\tau)|^2 \tilde{a}_3 \\
 & \quad + \frac{(1-\eta)}{r} [2(h_5 b_5^* + g_5 b_5 + a_5 k_5)] X(\tau)|Y(\tau)|^2 \tilde{a}_1 \\
 & \quad + [b_6^* ik h_6 + b_6 ik g_6 + k_6 ik a_6] X(\tau)|Y(\tau)|^2 \tilde{a}_3 \\
 & \quad + [h_4 b_3^* + b_4^* h_3 + g_4 b_3 + b_4 g_3 + a_3 k_4 + a_4 k_3] X(\tau)|Y(\tau)|^2 \tilde{a}_3 \\
 & \quad + \frac{(1-\eta)}{R_0 r} [-im h_4 b_5^* + b_4^* im h_5] X(\tau)|Y(\tau)|^2 \tilde{a}_1 \\
 & - \frac{1}{R_0^2} [b_6^* ik h_4 + b_6 ik g_4 + ik a_4 k_6] X(\tau)|Y(\tau)|^2 \tilde{a}_1 \\
 & \quad + \frac{2(1-\eta)}{R_0^2 r} [h_4 b_4^* + g_4 b_4 + a_4 k_4] X(\tau)|Y(\tau)|^2 \tilde{a}_1
 \end{aligned}$$

$$\begin{aligned}
 & + \frac{1}{R_0^2} [b_4^* ik h_6 + b_4 ik g_6 + ik a_6 k_4] X(\tau) |Y(\tau)|^{2\tilde{a}_1} \\
 & + \frac{(1-\eta)}{R_0 r} [im g_4 b_5 - im b_4 g_5] X(\tau) |Y(\tau)|^{2\tilde{a}_1}
 \end{aligned}$$

(ii) $\tilde{\underline{B}}^T \cdot$ (contribution from \underline{N}_1) =

$$\begin{aligned}
 & + \frac{(1-\eta)}{r} [2 d_5 b_5^* + 2k_5 b_5] Y(\tau) |Y(\tau)|^{2\tilde{b}_1} \\
 & - \frac{(1-\eta)}{R_0 r} [-im d_5 b_4^* + 2im b_5^* d_4 + k_5 im b_4] Y(\tau) |Y(\tau)|^{2\tilde{b}_1} \\
 & + [d_4 b_2^* + b_4^* d_2 + k_4 b_2 + b_4 k_2] Y(\tau) |Y(\tau)|^{2\tilde{b}_2} \\
 & + \frac{R_0(1-\eta)}{r} [-im d_5 b_5^* + 2im b_5^* d_5 + k_5 im b_5] Y(\tau) |Y(\tau)|^{2\tilde{b}_2} \\
 & + \frac{(1-\eta)}{r} [d_4 b_5^* + d_5 b_4^* + k_4 b_5 + b_4 k_5] Y(\tau) |Y(\tau)|^{2\tilde{b}_2} \\
 & + \frac{(1-\eta)R_0}{r} [-im d_5 b_6^* + 2im b_5^* d_6 + k_5 im b_6] Y(\tau) |Y(\tau)|^{2\tilde{b}_3} \\
 & + [d_4 b_3^* + b_4^* d_3 + k_4 b_3 + b_4 k_3] Y(\tau) |Y(\tau)|^{2\tilde{b}_3} \\
 & + \frac{(1-\eta)}{R_0 r} [-im d_4 b_5^* + 2im b_4^* d_5 + k_5 im b_5] X(\tau) |Y(\tau)|^{2\tilde{b}_1} \\
 & + \frac{2(1-\eta)}{R_0^2 r} [d_4 b_4^* + k_4 b_4] Y(\tau) |Y(\tau)|^{2\tilde{b}_1} \\
 & + \frac{2(1-\eta)}{r} [h_5 a_5^* + g_5^* a_5 + b_5 j_5] Y(\tau) |X(\tau)|^{2\tilde{b}_1}
 \end{aligned}$$

$$\begin{aligned}
 & - \frac{(1-\eta)}{R_0 r} [a_5^* \text{im } h_4 + a_5 \text{im } g_4^* + b_4 \text{im } j_5] Y(\tau) |X(\tau)|^{2\tilde{b}_1} \\
 & + [h_4 a_2^* + a_4^* h_2 + g_4^* a_2 + a_4 g_2^* + b_2 j_4 + b_4 j_2] Y(\tau) |X(\tau)|^{2\tilde{b}_2} \\
 & + \frac{(1-\eta)}{r} R_0 [a_5^* \text{im } h_5 + a_5 \text{im } g_5^* + \text{im } b_5 j_5] Y(\tau) |X(\tau)|^{2\tilde{b}_2} \\
 & + \frac{(1-\eta)}{r} [h_4 a_5^* + a_4^* h_5 + g_4^* a_5 + a_4 g_5^* + b_4 j_5 + b_5 j_4] Y(\tau) |X(\tau)|^{2\tilde{b}_2} \\
 & + [-1k h_6 a_5^* + a_6^* 1k h_5 + g_6^* 1k a_5 - 1k a_6 g_5^*] Y(\tau) |X(\tau)|^{2\tilde{b}_2} \\
 & \frac{(1-\eta)R_0}{r} [a_5^* \text{im } h_6 + a_5 \text{im } g_6^* + \text{im } j_5 b_6] Y(\tau) |X(\tau)|^{2\tilde{b}_3} \\
 & + \frac{2(1-\eta)}{R_0^2 r} [h_4 a_4^* + g_4^* a_4 + b_4 j_4] Y(\tau) |X(\tau)|^{2\tilde{b}_1} \\
 & + \frac{(1-\eta)}{R_0 r} [a_4^* \text{im } h_5 + a_4 \text{im } g_5^* + \text{im } b_5 j_4] Y(\tau) |X(\tau)|^{2\tilde{b}_1} \\
 & + \frac{1}{R_0^2} [-1k h_4 a_6^* + a_4^* 1k h_6 + g_4^* 1k a_6 - 1k a_4 g_6^*] Y(\tau) |X(\tau)|^{2\tilde{b}_1} \\
 & - \frac{1}{R_0^2} [-1k h_6 a_4^* + a_6^* 1k h_4 + g_6^* 1k a_4 - 1k a_6 g_4^*] Y(\tau) |X(\tau)|^{2\tilde{b}_1} \\
 & + [h_4 a_3^* + a_4^* h_3 + g_4^* a_3 + a_4 g_3^* + b_3 j_4 + b_4 j_3] Y(\tau) |X(\tau)|^{2\tilde{b}_3}.
 \end{aligned}$$

REFERENCES

- BOYCE, W. E. & DIPRIMA, R. C. (1977): Elementary Differential Equations and Boundary Value Problems, Wiley.
- DEAN, W. R. (1928): "Fluid motion in a curved channel," Proc. Roy. Soc. (A), A121, pp. 402-440.
- EAGLES, P. M. (1971): "On stability of Taylor vortices by fifth-order amplitude expansions," J. Fluid Mech., Vol. 49, pp. 529-550.
- GIBSON, R. E. & COOK, A. E. (1974): "The stability of curved channel flow," Quart. J. Mech. Appl. Math., Vol. 27, pp. 149-160.
- GUCKENHEIMER, J. & HOLMES, P. (1963): Nonlinear Oscillations, Dynamical Systems, and Bifurcations of Vector Fields, Springer.
- HALL, P. & SMITH, F. T. (1984): "On the effects of nonparallelism, three-dimensionality and mode interaction in nonlinear boundary layer stability," Stud. Appl. Math., pp. 91-120.
- HALL, P. & MALIK, M. (1986): "On the instability of a three-dimensional attachment line boundary layer: Weakly nonlinear theory and a numerical approach," J. Fluid Mech., Vol. 163, p. 257.
- KEENER, J. P. (1976): "Secondary bifurcation in nonlinear diffusion reaction equations," Stud. Appl. Math., Vol. 55, pp. 187-211.

- MALIK, M., CHUANG, S., & HUSSAINI, M. Y. (1982): "Accurate numerical solution of compressible linear stability equations," ZAMP, Vol. 33, pp. 189-201.
- MATKOWSKY, B. J. (1970): "Nonlinear dynamic stability: A formal theory," SIAM J. Appl. Math., Vol. 18, pp. 872-883.
- MEKSYN, D. & STUART, J. T. (1951): "Stability of viscous motion between parallel plates for finite disturbances," Proc. Roy. Soc. (A), Vol. 208, pp. 517-526.
- ORSZAG, S. (1971): "Accurate solution of the Orr-Sommerfeld stability equation," J. Fluid Mech., Vol. 50, pp. 689-703.
- SMITH, F. T. (1979): "Nonlinear stability of boundary layers for disturbances of various sizes," Proc. Roy. Soc. (A), Vol. 368, pp. 573-589.
- STUART, J. T. (1958): "On the nonlinear mechanics of hydrodynamic stability," J. Fluid Mech., Vol. 4, pp. 1-21.
- TAYLOR, G. I. (1923): "Stability of a viscous liquid contained between two rotating cylinders," Philos. Trans. Roy. Soc. (A), Vol. A223, pp. 289-343.
- WALOWIT, J., TSAO, S., & DIPRIMA, R. C. (1964): "Stability of flow between arbitrary spaced concentric cylindrical surfaces including the effect of a radial temperature gradient," J. Appl. Mech., Vol. 31, pp. 585-593.

FIGURE CAPTIONS

- Figure 1 Curved channel with flow in the azimuthal direction. The walls are parallel to the z-axis. Radius ratio $\eta = R_1/R_0$ and channel width $d = R_0 - R_1$.
- Figure 2 Critical Reynolds number versus $(1 - \eta)$ for Görtler and TS perturbations. At the cross-over point of these curves, $Re_c = 8 \times 5772.2$ and $(1 - \eta_c) = 2.179 \times 10^{-5}$. This figure is a schematic adaptation of Figure 1 in Gibson & Cook (1974).
- Figure 3 Neutral stability curve for the Görtler perturbation. Reynolds number versus axial wave number k .
- Figure 4 Neutral stability curve for the Tollmien-Schlichting perturbation. Reynolds number versus azimuthal wavenumber m .
- Figure 5 The two neutral stability curves (a) Görtler neutral stability curve (b) TS neutral stability curve for $\eta = \eta_c$. For this case, the critical Reynolds number is identical for the two perturbations. GL and GU refer to the lower and upper arms of the Görtler stability curve. TSL and TSU refer to the lower and upper arms of the Tollmien-Schlichting stability curve.
- Figure 6 Reynolds number versus growth rate β_1 of the Görtler perturbation.
- Figure 7 Reynolds number versus growth rate β_2 of the TS perturbation. Note the negative β_2 for part of TSU.
- Figure 8 Reynolds number versus η_1 for perturbations corresponding to the two arms GL and GU of the Görtler stability curve interacting with TSL and TSU:

- (a) GL interacting with TSL and TSU.
- (b) GU interacting with TSL and TSU.

Figure 9 Reynolds number versus δ_2 for perturbations corresponding to the two arms GL and GU of the Görtler stability curve interacting with TSL and TSU:

- (a) GL interacting with TSL and TSU.
- (b) GU interacting with TSL and TSU.

Figure 10 Reynolds number versus η_2 .

Figure 11 Bifurcation diagrams for the interaction of the Görtler and TS perturbations for Reynolds number at or close to Re_c where

$$\eta_1/\eta_2 > \beta_1/\beta_2 > \delta_1/\delta_2$$

and

$$\eta_i > 0, \beta_i > 0, \delta_i < 0, i = 1, 2.$$

(a) ($\nu > 0$). The Görtler mode is the most linearly unstable mode in this case. The TS mode is subcritically unstable.

(b) ($\nu < 0$). The values of μ at P and Q are respectively

$$\mu_P = \frac{-\nu\gamma_1/\beta_1}{\left(1 - \frac{\eta_1}{\eta_2} \frac{\beta_2}{\beta_1}\right)}$$

and

$$\mu_Q = \frac{-\nu\gamma_1/\beta_1}{\left(1 - \frac{\delta_1}{\delta_2} \frac{\beta_2}{\beta_1}\right)}.$$

Figure 12 Bifurcations diagrams for the interaction of GL and TSL where

$$\eta_1/\eta_2 > \beta_1/\beta_2 > \delta_1/\delta_2$$

and

$$\eta_i < 0, \beta_i > 0, \delta_i < 0, i = 1, 2.$$

(a) ($\nu < 0$). The TS mode is the most linearly unstable mode in this case. The value of μ at Q is

$$\mu_Q = \frac{-\nu\gamma_1/\beta_1}{\left(1 - \frac{\delta_1}{\delta_2} \frac{\beta_1}{\beta_2}\right)} .$$

(b) ($\nu > 0$). The Gortler mode is the most linearly unstable mode in this case. The value of μ at P is

$$\mu_P = \frac{-\nu\gamma_1/\beta_1}{\left(1 - \frac{\eta_1}{\eta_2} \frac{\beta_2}{\beta_1}\right)} .$$

Figure 13 Bifurcation diagrams for the interaction of GU and TSL where

$$-\eta_1/\eta_2 > \beta_1/\beta_2 > \delta_1/\delta_2$$

and

$$\eta_1 > 0, \eta_2 < 0, \beta_i > 0, \delta_i < 0, i = 1, 2.$$

(a) ($\nu < 0$). The TS is the most linearly unstable mode in this case. The values of μ at P and Q are respectively:

$$\mu_P = \frac{-\nu\gamma_1/\beta_1}{\left(1 - \frac{\eta_1}{\eta_2} \frac{\beta_2}{\beta_1}\right)}$$

and

$$\mu_Q = \frac{-\nu\gamma_1/\beta_1}{\left(1 - \frac{\delta_1}{\delta_2} \frac{\beta_2}{\beta_1}\right)} .$$

(b) ($\nu > 0$). The Gortler mode is the most linearly unstable mode in this case.

LIST OF TABLES

Table 1

Coefficients of the Landau equations are listed for the four possible interactions under Sections A, B, C, and D. The first three columns list the Reynolds number R_0 , wave number k of the Görtler and wave number m of the TS waves respectively. These are values on the neutral stability curves for the Görtler and TS perturbations. The remaining columns list the coefficients of the Landau equations and some of their ratios.

Section A: Interaction of TSL with GL

Section B: Interaction of TSL with GU

Section C: Interaction of TSU with GL

Section D: Interaction of TSU with GU

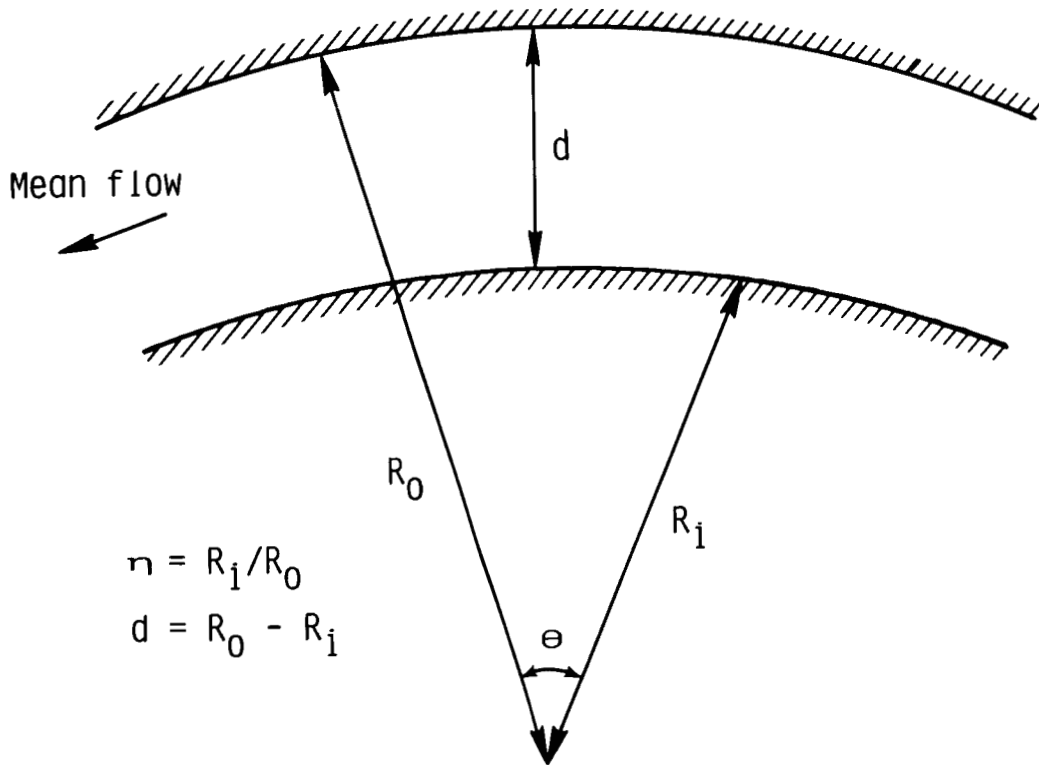


Figure 1

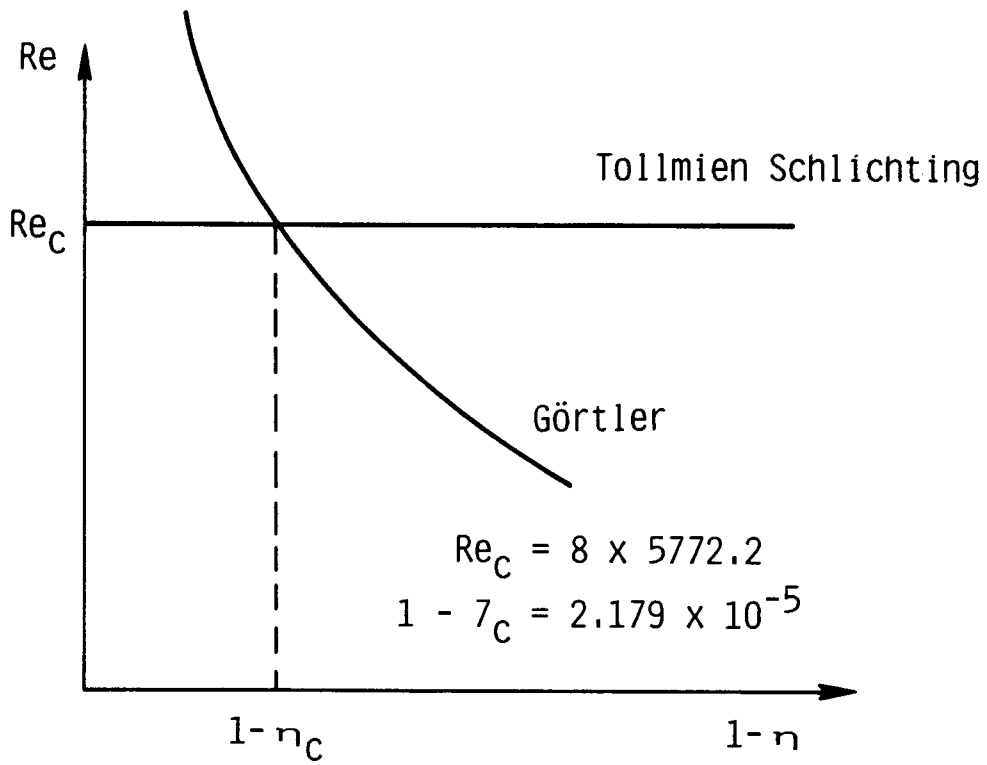


Figure 2

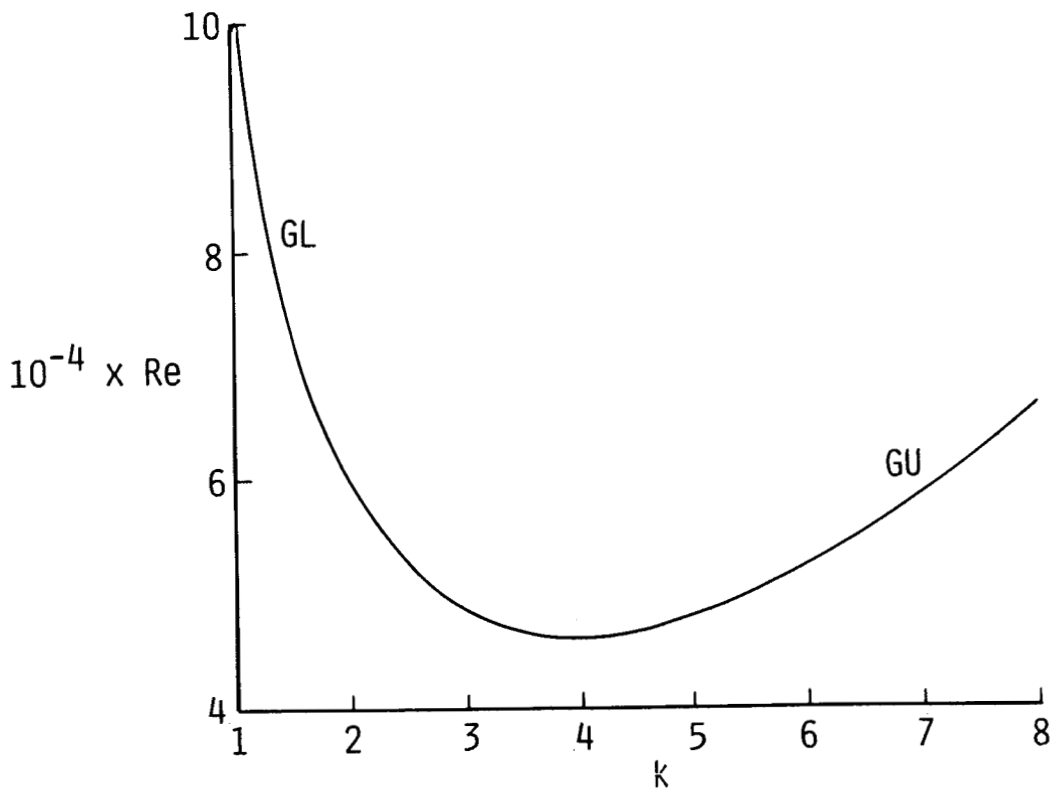


Figure 3

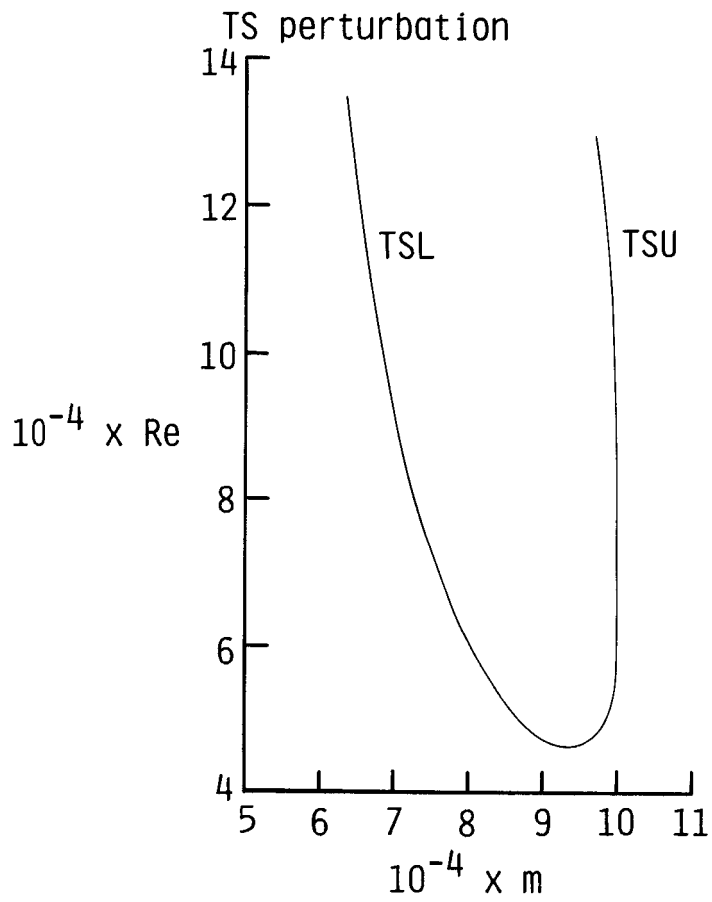


Figure 4

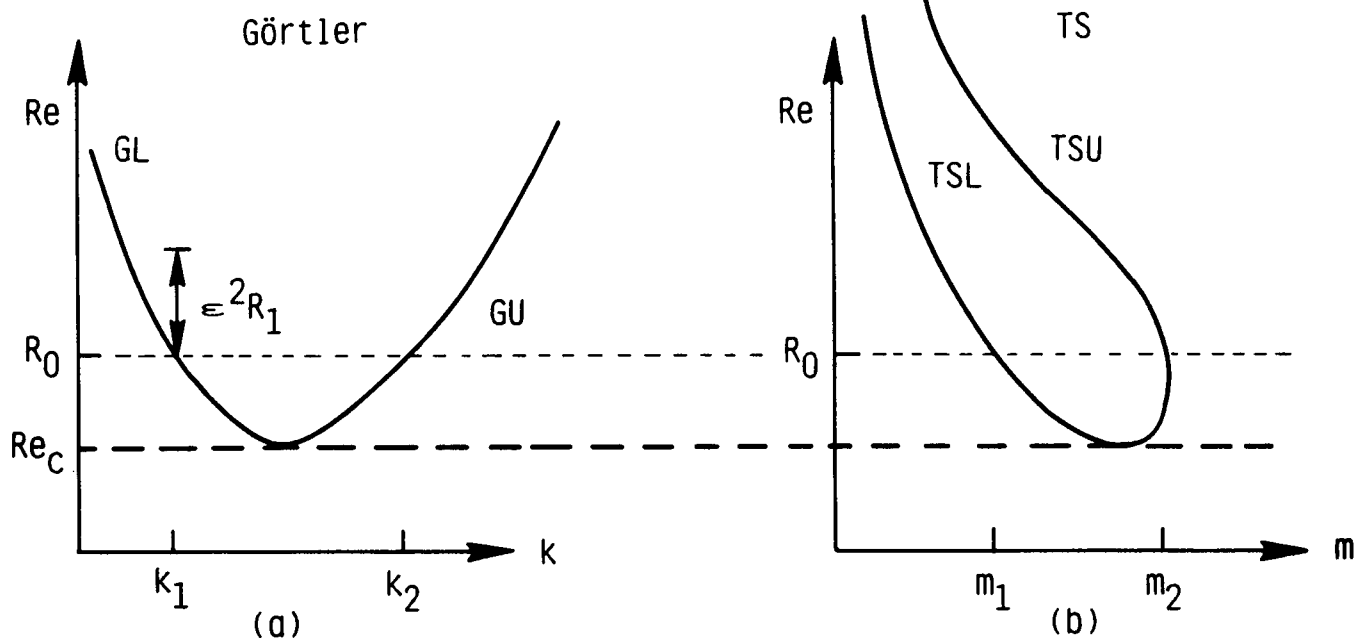


Figure 5

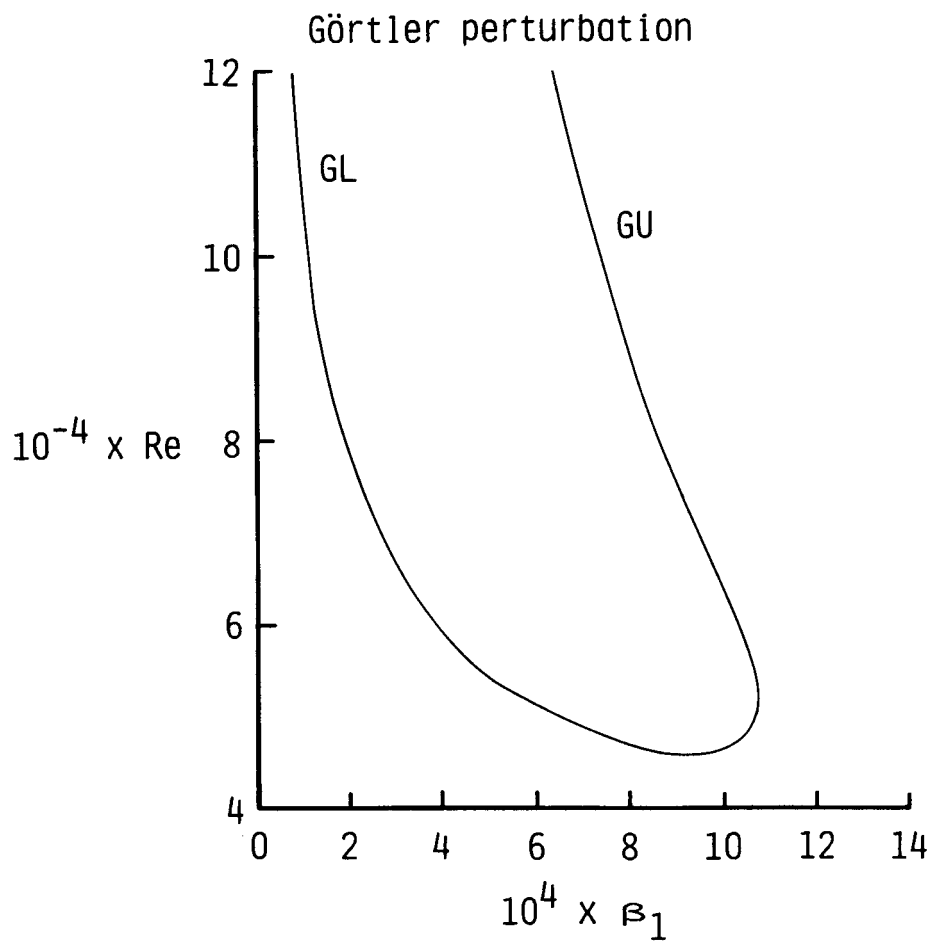


Figure 6

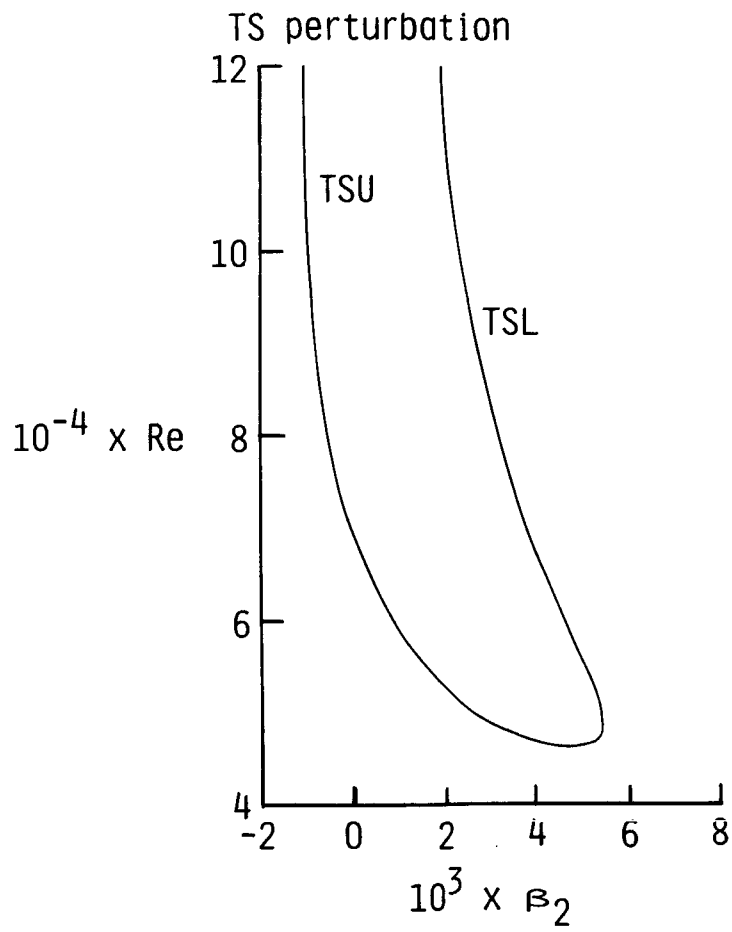


Figure 7

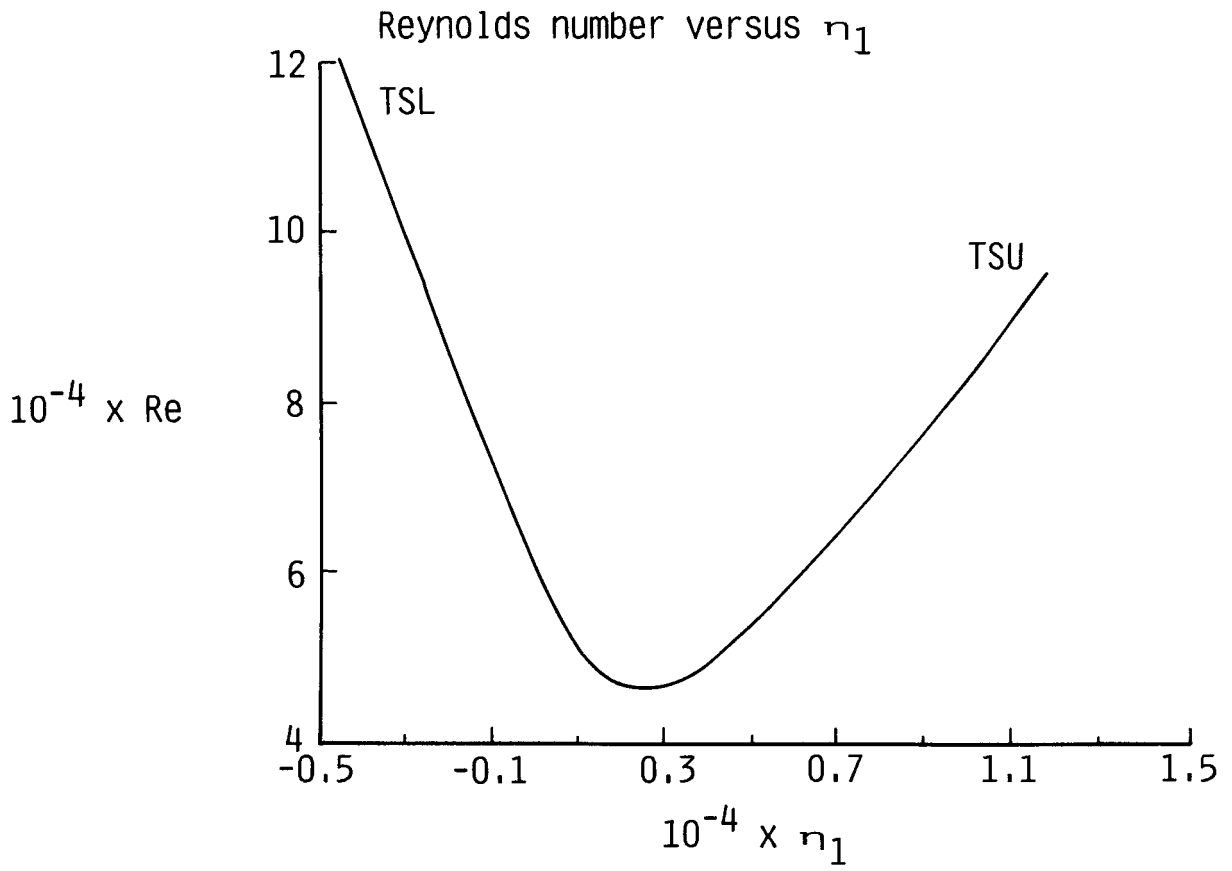


Figure 8a

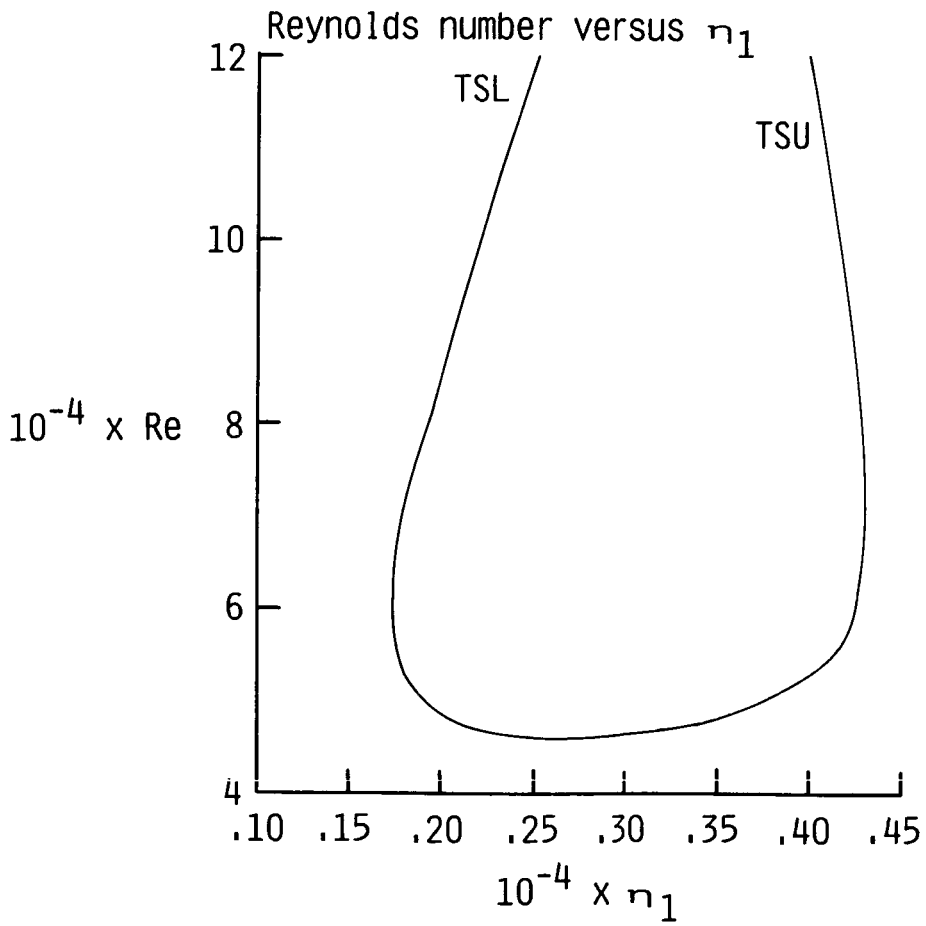


Figure 8b

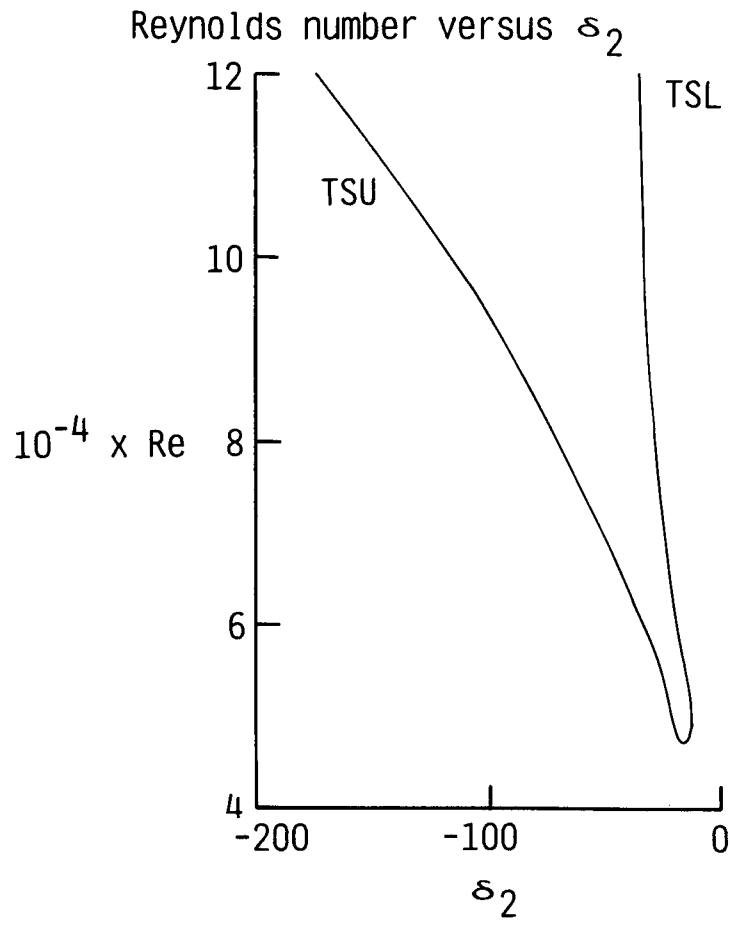


Figure 9a

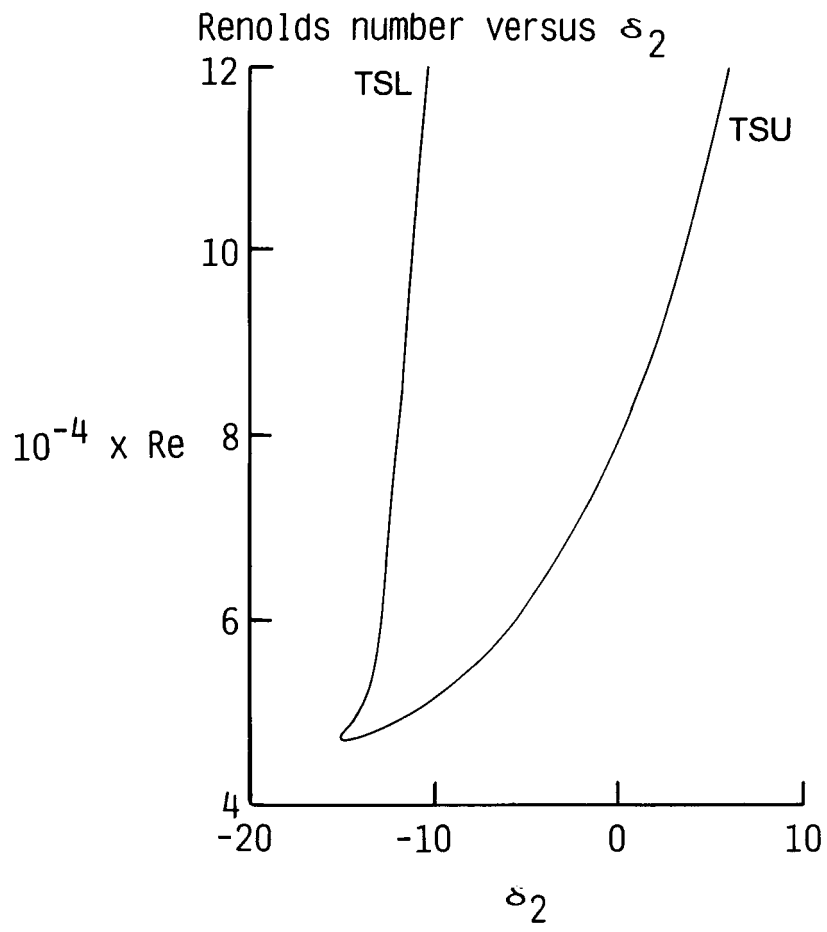


Figure 9b

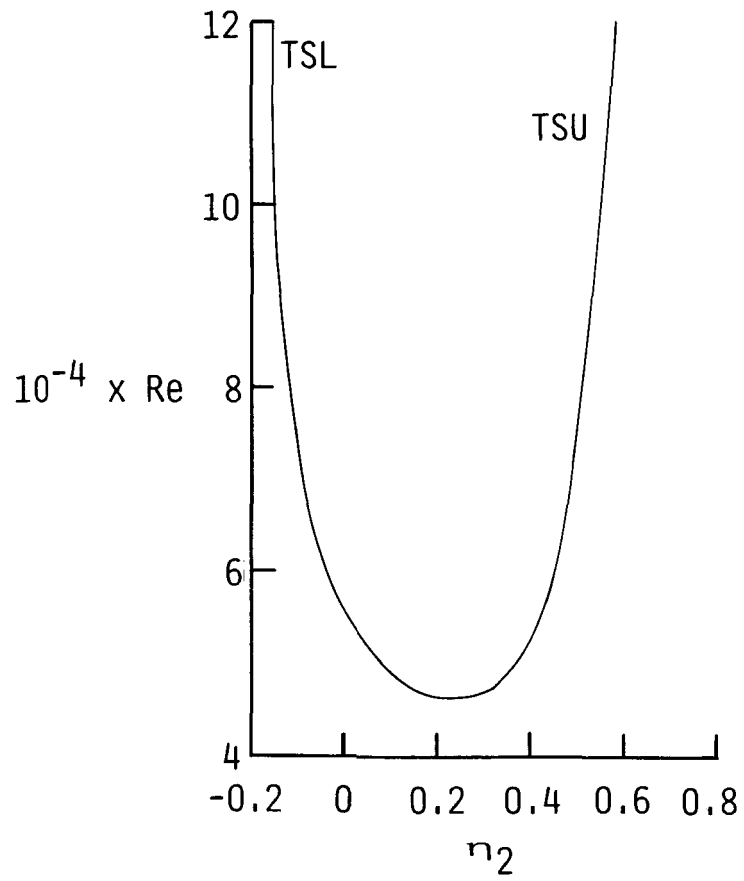


Figure 10

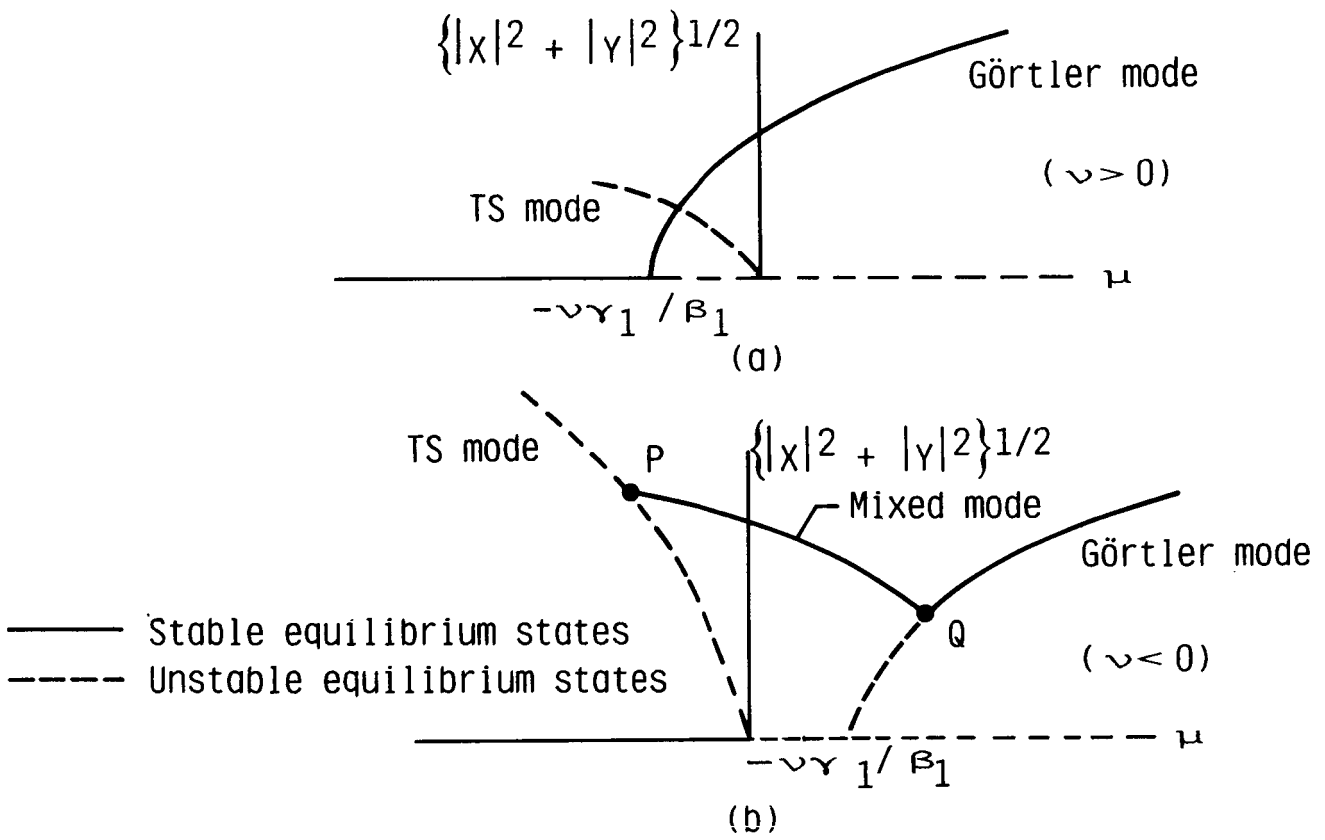


Figure 11

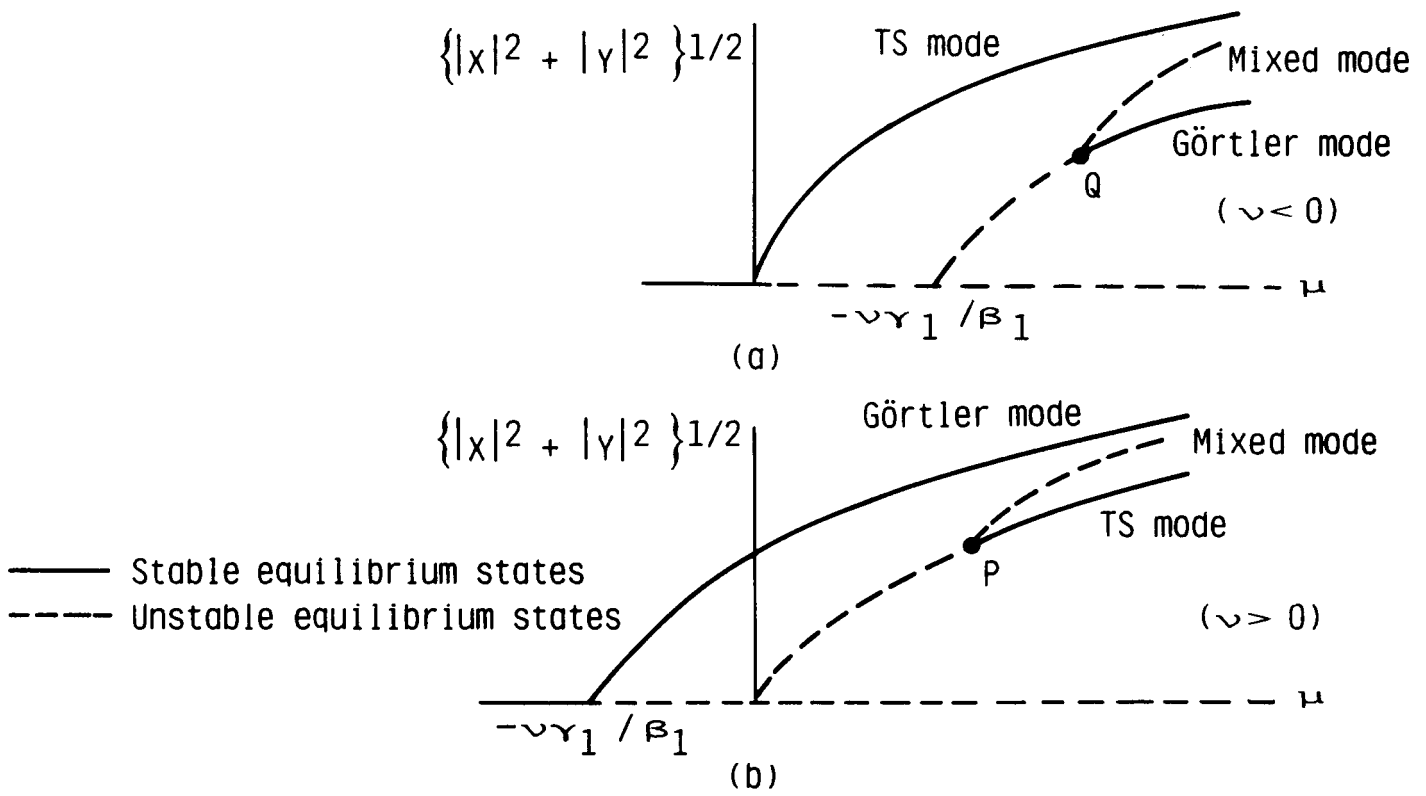


Figure 12

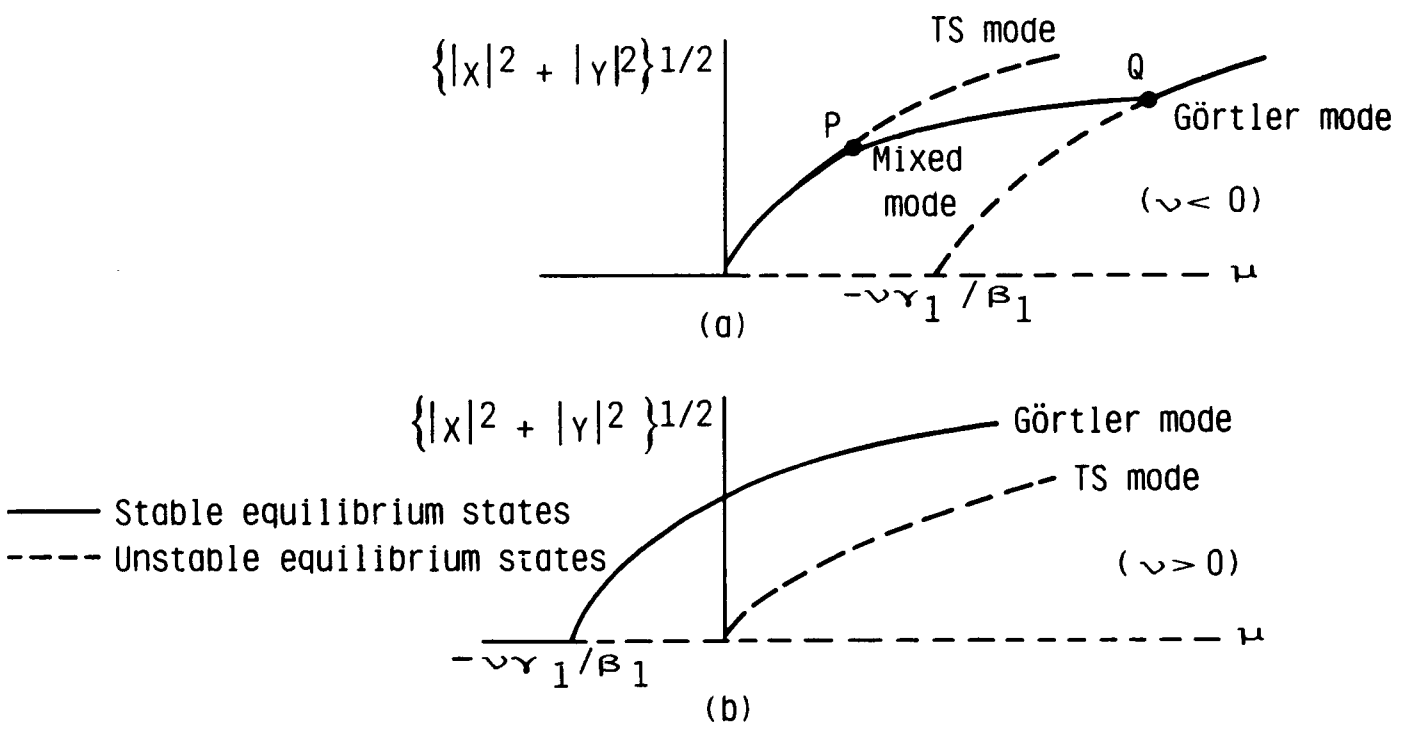


Figure 13

TABLE 1

	Reynolds number R_0	k	m	β_1	δ_1	η_1	β_2	η_2	δ_2	δ_1/δ_2	η_1/η_2	β_1/β_2
Section A	.120(6)	.855	.656(5)	.83(-4)	-1.0	-.45(4)	.19(-2)	-.16	-.36(2)	.28(-1)	.27(5)	.43(-1)
	.800(5)	1.35	.732(5)	.20(-3)	-1.0	-.15(4)	.33(-2)	-.12	-.28(2)	.35(-1)	.13(5)	.60(-1)
	.700(5)	1.60	.762(5)	.26(-3)	-1.0	-.79(3)	.39(-2)	-.89(-1)	-.25(2)	.39(-1)	.88(4)	.68(-1)
	.675(5)	1.67	.771(5)	.29(-3)	-1.0	-.59(3)	.40(-2)	-.79(-1)	-.25(2)	.41(-1)	.75(4)	.71(-1)
	.625(5)	1.86	.791(5)	.35(-3)	-1.0	-.17(3)	.44(-2)	-.53(-1)	-.23(2)	.44(-1)	.31(4)	.78(-1)
	.600(5)	1.98	.803(5)	.38(-3)	-1.0	.63(2)	.46(-2)	-.37(-1)	-.21(2)	.47(-1)	-.17(4)	.83(-1)
	.575(5)	2.11	.816(5)	.43(-3)	-1.0	.31(3)	.48(-2)	-.18(-1)	-.20(2)	.51(-1)	-.17(5)	.88(-1)
	.550(5)	2.27	.830(5)	.48(-3)	-1.0	.59(3)	.51(-2)	.53(-2)	-.18(2)	.56(-1)	.11(6)	.94(-1)
	.480(5)	3.08	.891(5)	.73(-3)	-1.0	.17(4)	.54(-2)	.12	-.43(2)	.24(-1)	.14(5)	.13
	.468(5)	3.44	.911(5)	.82(-3)	-1.0	.21(4)	.53(-2)	.17	-.25(2)	.41(-1)	.13(5)	.15
Section B	.120(6)	12.9	.656(5)	.64(-3)	-1.0	.25(4)	.19(-2)	-.16	-.10(2)	.96(-1)	-.15(5)	.33
	.100(5)	11.3	.688(5)	.74(-3)	-1.0	.22(4)	.24(-2)	-.15	-.11(2)	.90(-1)	-.15(5)	.30
	.750(5)	9.02	.746(5)	.91(-3)	-1.0	.19(4)	.36(-2)	-.11	-.12(2)	.82(-1)	-.18(5)	.26
	.600(5)	7.23	.803(5)	.10(-2)	-1.0	.17(4)	.46(-2)	-.37(-1)	-.13(2)	.77(-1)	-.46(5)	.22
	.550(5)	6.47	.830(5)	.11(-2)	-1.0	.18(4)	.51(-2)	.53(-2)	-.13(2)	.75(-1)	.33(6)	.21
	.500(5)	5.52	.868(5)	.11(-2)	-1.0	.19(4)	.54(-2)	.74(-1)	-.14(2)	.70(-1)	.25(5)	.20
.470(5)	4.64	.963(5)	.10(-2)	-1.0	.32(4)	.40(-2)	.30	-.15(2)	.66(-1)	.11(5)	.26	
Section C	.120(6)	.855	.983(5)	.83(-4)	-1.0	.15(5)	-.11(-2)	.55	-.17(3)	.58(-2)	.28(5)	-.76(-1)
	.900(5)	1.18	.100(6)	.15(-3)	-1.0	.11(5)	-.81(-3)	.53	-.91(2)	.11(-1)	.21(5)	-.19
	.700(5)	1.60	.101(6)	.26(-3)	-1.0	.79(4)	-.63(-4)	.49	-.51(2)	.20(-1)	.16(5)	-.42(1)
	.650(5)	1.76	.101(6)	.31(-3)	-1.0	.71(4)	.31(-3)	.48	-.43(2)	.24(-1)	.15(5)	.10(1)
	.470(5)	3.35	.963(5)	.80(-3)	-1.0	.33(4)	.40(-2)	.30	-.28(2)	.36(-1)	.11(5)	.20
Section D	.120(6)	12.9	.983(5)	.64(-3)	-1.0	.40(4)	-.11(-2)	.55	.60(1)	-.17	.73(4)	-.58
	.100(5)	11.3	.995(5)	.74(-3)	-1.0	.42(4)	-.96(-3)	.54	.35(1)	-.28	.77(4)	-.77
	.800(5)	9.53	.101(6)	.87(-3)	-1.0	.43(4)	-.54(-3)	.51	.37(-1)	-.27(2)	.87(4)	-.16(1)
	.500(5)	5.52	.985(5)	.11(-2)	-1.0	.38(4)	.28(-2)	.37	-.12(2)	.87(-1)	.10(5)	.39
	.470(5)	4.64	.963(5)	.10(-2)	-1.0	.32(4)	.40(-2)	.30	-.15(2)	.66(-1)	.11(5)	.26

Standard Bibliographic Page

1. Report No. NASA CR-178286 ICASE Report No. 87-26		2. Government Accession No.		3. Recipient's Catalog No.	
4. Title and Subtitle ON THE NONLINEAR INTERACTION OF GORTLER VORTICES AND TOLLMIE-SCHLICHTING WAVES IN CURVED CHANNEL FLOWS AT FINITE REYNOLDS NUMBERS				5. Report Date April 1987	
				6. Performing Organization Code	
7. Author(s) Q. Isa Daudpota, Philip Hall, and Thomas A. Zang				8. Performing Organization Report No. 87-26	
				10. Work Unit No.	
9. Performing Organization Name and Address Institute for Computer Applications in Science and Engineering Mail Stop 132C, NASA Langley Research Center Hampton, VA 23665-5225				11. Contract or Grant No. NAS1-17070, NAS1-18107	
				13. Type of Report and Period Covered Contractor Report	
12. Sponsoring Agency Name and Address National Aeronautics and Space Administration Washington, D.C. 20546				14. Sponsoring Agency Code 505-90-21-01	
				15. Supplementary Notes Langley Technical Monitor: Submitted to the J. Fluid Mech. J. C. South Final Report	
16. Abstract The flow in a two-dimensional curved channel driven by an azimuthal pressure gradient can become linearly unstable due to axisymmetric perturbations and/or nonaxisymmetric perturbations depending on the curvature of the channel and the Reynolds number. For a particular small value of curvature, the critical Reynolds number for both these perturbations becomes identical. In the neighborhood of this curvature value and critical Reynolds number, nonlinear interactions occur between these perturbations. The Stuart-Watson approach is used to derive two coupled Landau equations for the amplitudes of these perturbations. The stability of the various possible states of these perturbations is shown through bifurcation diagrams. Emphasis is given to those cases which have relevance to external flows.					
17. Key Words (Suggested by Authors(s)) nonlinear wave interaction, stability theory, curved channel flows			18. Distribution Statement 02 - Aerodynamics 34 - Fluid Mechanics and Heat Transfer Unclassified - unlimited		
19. Security Classif.(of this report) Unclassified		20. Security Classif.(of this page) Unclassified		21. No. of Pages 62	22. Price A04

For sale by the National Technical Information Service, Springfield, Virginia 22161